



ORIGINAL ARTICLE

Novel indan-1,3-dione derivatives: Design, green synthesis, effect against tomato damping-off disease caused by *Fusarium oxysporum* and in silico molecular docking study



Khairiah Nasser AL-Shammri ^a, Nadia A.A. Elkanzi ^{a,b,*}, Wael A.A. Arafa ^{a,c}, Ibrahim O. Althobaiti ^d, Rania B. Bakr ^e, Shaima Mohamed Nabil Moustafa ^{f,g}

^a Chemistry Department, College of Science, Jouf University, P.O. Box: 2014, Sakaka, Saudi Arabia

^b Chemistry Department, Faculty of Science, Aswan University, P.O. Box: 81528, Aswan, Egypt

^c Chemistry Department, Faculty of Science, Fayoum University, P.O. Box 63514, Fayoum, Egypt

^d Department of Chemistry, College of Science and Arts, Jouf University, Saudi Arabia

^e Department of Pharmaceutical Organic Chemistry, Faculty of Pharmacy, Beni-Suef University, Beni-Suef 62514, Egypt

^f Biology Department, College of Science, Jouf University, Sakaka 2014, Saudi Arabia

^g Department of Botany and Microbiology, Faculty of Science, Minia University, El-Minia 61511, Egypt

Received 12 December 2021; accepted 23 January 2022

Available online 3 February 2022

KEYWORDS

Pyrazole derivatives;
Chalcones;
Green synthesis;
Antifungal activity;
Molecular docking

Abstract An effective method for synthesizing series of twenty-two new compounds **1**, **2a,b**, **3**, **4a**, **b**, **5a-e**, **7**, **8**, **9**, **10**, **12**, **13a-d**, **15a,b** was performed starting from reaction of 1,2,3-indenetrione thiourea, and ethyl cyanoacetate under microwave irradiation and / or 2-(1,3-dioxo-1*H*-inden-2(3*H*)-ylidene) hydrazine carbothioamide with acetic anhydride. Chemical structure of the obtained products has been established by spectroscopic techniques including FTIR, ¹H NMR, ¹³C NMR, DEPT-135, and mass spectroscopy. The designed new compounds have been successfully examined *in-vitro* for their antifungal activities. The relation between the structure of the synthesized compounds and their activity against tomato damping-off disease caused by *Fusarium oxysporum* fungi was studied and favourable results were obtained. The antifungal studies indicated that compounds **1**, **7**, **4a** and **5a-d** exerted the highest antifungal activities, while **3** and **4b** recorded the lowest effect. The obtained results confirmed the possibility of the application of ethyl 6'-amino-1,3-dioxo-2'-th

* Corresponding author at: Chemistry Department, College of Science, Jouf University, P.O. Box: 2014, Sakaka, Saudi Arabia.

E-mail address: nahasan@ju.edu.sa (N.A.A. Elkanzi).

Peer review under responsibility of King Saud University.



ioxo-1,2',3,3'-tetrahydro-1'*H*-spiro[indene-2,4'-pyrimidine]-5'-carboxylate **1** as a new effective regulator of the vegetative growth of tomatoes. The molecular docking analysis was performed within succinate dehydrogenase (SDH) as a target enzyme in order to rationalize the promising findings obtained for the active compounds **1**, **2a,b**, **5a-d**, **7**, **8**, **9**, **10**, **12**, and **13a**.

© 2022 The Author(s). Published by Elsevier B.V. on behalf of King Saud University. This is an open access article under the CC BY license (<http://creativecommons.org/licenses/by/4.0/>).

1. Introduction

Pesticides are efficient means for protecting crops growing agricultural yields, within which fungicides exhibiting an essential role in modern agriculture (Kumar et al., 2019; (Shang et al., 2019)). Due to the emergence of fungicide-resistance issues, it is essential to develop new antifungal agents with high efficiency and more selectivity. On the other hand, tomato (*Solanum lycopersicum* L.) is one of widely cultivated crops in different countries (Srivastava et al., 2010; (McGovern, 2015; (Kaiwart et al., 2020)), Tomato are parasitized by different pathogenic bacteria, viruses, fungi and nematodes which are constraints to tomato farming such as tomato leaf curl disease, *Fusarium* wilt, bacterial wilt, *Verticillium* wilt and damping off (Al-ani et al., 2011; (Karthika et al., 2020; (Campos et al., 2021)). Damping-off disease is one of the worst diseases of tomato, which can kill germinating seeds and young seedlings also (Lamichhane et al., 2017). *Fusarium* is soil borne pathogenic fungi, and the main prevalent, serious diseases of tomatoes that causes loss in tomato production in both field and greenhouse (Maurya et al., 2019). Several disease management strategies are available e.g. chemical control (Abo-Elyour and Mohamed, 2009), using chloropicrin and methyl-bromide (McGovern et al., 1998) and inducing resistance in susceptible tomato plants via utilizing CuCl₂ and MnSO₄ (Mandal and Sinha, 1992). In 2020, symptoms of damping-off disease of tomato were shown in a field of Al-Jouf region, KSA. A diseased seedling was observed damping-off in which the fungus attacked the basal part of the stems and finally led to collapse of the plant on the soil surface. Many bare areas appeared in the diseased fields (see Fig. 1).

It was documented that heterocycles comprising indane-1,3-diones attracted considerable interest because of their diverse biological potentials as antiviral (Oliveira et al., 2018; (de Oliveira et al., 2019)), α -glucosidase inhibitors (Mukhtar et al., 2021), A β ₁₋₄₀ fibrillogenesis inhibitor (Catto et al., 2010), antioxidant (Kouzi et al., 2019), anti-inflammatory (Giles et al., 2011; (A Muhammad et al., 2017)), antiparkinson (Millan et al., 2004), urease inhibitor (Bano et al., 2018) and antifungal (Sarvesh and Nizamuddin, 2008; (Xu et al., 2009; (Mohil et al., 2014; (Meena et al., 2017)). 4-Hydroxyphenylmethylene-indane-1,3-dione **A** was found to exert comparable antifungal effect towards *A. niger* (zone of inhibition = 23 mm) and *C. albicans* (zone of inhibition = 25 mm) to that recorded by griseofulvin (zone of inhibition = 26 and 24 mm, respectively) (Meena et al., 2017). Furthermore, the indeno derivative **B** revealed comparable zone of inhibition towards *A. niger* (inhibition zone = 29.65 mm) to that recorded by fluconazole (inhibition zone = 31.80 mm) at concentration 100 μ g/mL (Patel et al., 2012). Heterocyclic compounds incorporating pyrimidine nucleus draw the

attention of medicinal chemists owing to its versatile biological roles as anti-inflammatory (Abdelgawad et al., 2018; (Abdelgawad et al., 2019)), anticancer (Al-Sanea et al., 2020; (Ghoneim et al., 2020)), antidiabetic (Panahi et al., 2013), protein kinase inhibitor (B Bakr et al., 2017; (Abdellatif and Bakr, 2020)), antimicrobial (Bakr et al., 2018; (Radwan et al., 2020; (Zhuang and Ma, 2020)) and antifungal (Liu et al., 2005; (Maddila et al., 2016; (Sheikhi-Mohammareh et al., 2020)). For example, pyrimidin-4-yl-oxy-phenylbenzamide derivative **C** recorded antifungal potential against *Phomopsis* Sp. with EC₅₀ = 1.4 μ g/mL which is more potent than pyrimethanil (EC₅₀ = 32.1 μ g/ml) (Wu et al., 2019). In addition, pyrimidine derivative **D** (MIC = 12.5 μ g/ml) showed the same antifungal activity towards *C. albicans* as the standard drug Clotrimazole (MIC = 12.5 μ g/ml) (Sharshira and Hamada, 2012). Moreover, thiadiazole incorporating heterocycles recorded antifungal potential (Keerthi Kumar et al., 2013; (Fadda et al., 2017)). For instance, thiadiazole compound **E** (zone of inhibition = 25 mm) exhibited higher antifungal potency towards *C. albicans* than fluconazole (zone of inhibition = 22 mm) (El-Naggar et al., 2019). Prompted by all of these facts and in continuation of our work aiming at discovering novel antimicrobial agents (Bakr et al., 2018; (Ghoneim et al., 2018; (Elkanzi et al., 2019a; (Elkanzi et al., 2019b; (Bakr and Elkanzi, 2020; (Elkanzi and Bakr, 2020; (Elkanzi et al., 2020; (Ghoneim et al., 2020; (Hrichi et al., 2020)), We report herein hybridizing the indane-1,3-dione scaffold with pyrimidine and/or thiadiazole heterocycles to get novel antifungal agents. To explore the antifungal potential of these newly prepared compounds, zones of inhibition of these compounds were estimated towards *Fusarium oxysporum* testing their effects on tomato seed germination. Furthermore, in silico molecular docking study had been conducted for the novel candidates within succinate dehydrogenase enzyme in an attempt to predict the binding mode of these novel compounds as antifungal agents. The objective of this study was to isolate and identifying causal organisms of tomato damping off disease based on the pathogens morphological and molecular characterization.

2. Experimental

2.1. Chemistry

All chemical reagents used for synthesis were purchased from Sigma Aldrich (Somatco Trading Co. Ltd., Sakaka, Aljouf, Saudi Arabia) and used without further purification. The reaction progress was controlled using thin layer chromatography (TLC) on silica gel pre-coated F254Merck plates (Darmstadt, Germany). The visualization of spots was performed with ultraviolet irradiation at 350–380 nm. Melting points (m.p.) of the synthesized compounds were determined on a Galenkamp electrothermal melting point apparatus and are

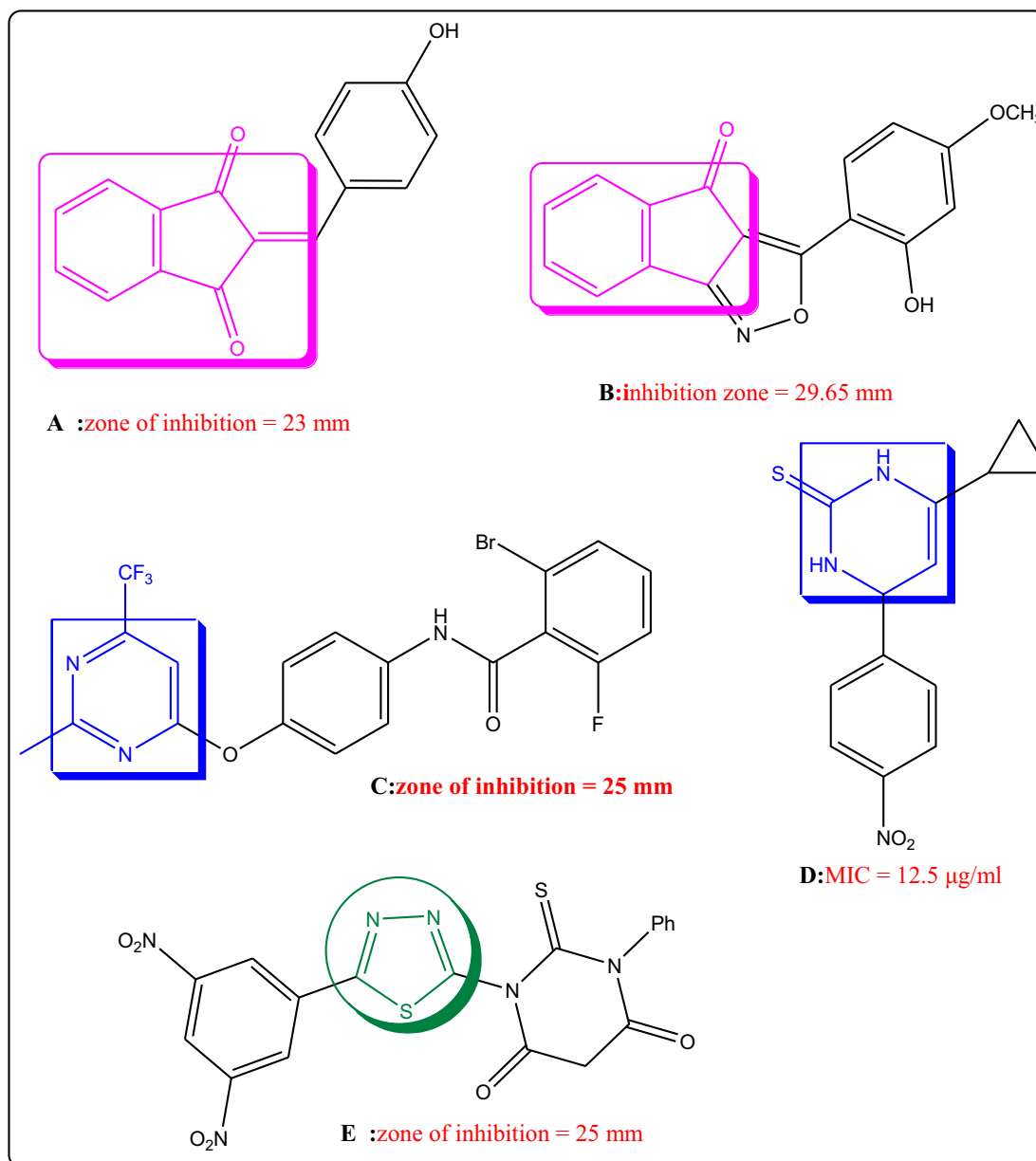


Fig. 1 Examples of indane-1,3-diones (**A**, **B**), pyrimidines (**C**, **D**) and thiadiazole (**E**) with antifungal potential.

uncorrected. The elemental analyses (C, H, and N) of the synthesized compounds were realized on CE 440 Elemental Analyzer- Automatic Injector (Exeter Analytical, Inc., USA) at the Microanalytical Center of Cairo University. IR spectra were registered on Shimadzu infrared spectrophotometer (Chemistry department research laboratory, Jouf University) using potassium bromide disks. ^1H , ^{13}C NMR spectra were recorded on a Varian MercuryVXR-300 NMR spectrometer (Palo Alto, CA) at 400 and 125 MHz in dimethyl sulfoxide- d_6 (DMSO d_6) and DEPT-135 (ppm). The chemical shifts are given in ppm (δ) relative to the internal standard TMS. DEPT-135 was used; Mass spectra were obtained at 70 eV on a shimadzu GCMS-QP 1000EX spectrometer. Microwave irradiations were carried out in a Kenstar OM9925E MW oven (2450 MHz, 800 W). Ultrasonic irradiation was performed in an ELO-150 ultrasonic cleaner with a frequency of 46 kHz and a nominal power of 200 W.

2.1.1. Synthesis of ethyl 6'-amino-1,3-dioxo-2'-thioxo-1,2',3,3'-tetrahydro-1'H-spiro[indene-2,4'-pyrimidine]-5'-carboxylate (**1**)

a) Conventional method:

A mixture of thiourea (1.0 mmol), ethyl cyano acetate (1.0 mmol), 1, 2, 3-indenetrione (1.0 mmol) and potassium carbonate (1.0 mmol) in absolute ethanol (50.0 mL) was refluxed for 8 h. The reaction was monitored by thin-layer chromatography (TLC). After completion of the reaction, the reaction mixture was neutralized with concentrated hydrochloric acid, and the precipitate was filtered and recrystallized from ethanol.

b) Microwave method:

A mixture of thiourea (1.0 mmol), ethyl cyanoacetate (1.0 mmol), 1, 2, 3-indenetrione (1.0 mmol) and potassium car-

bonate (a catalytic amount) was taken in about 30.0 mL of ethanol (one pot reaction). The reaction mixture was subjected to microwave for about 20 min. TLC monitored the completion of reaction, and the product was obtained in the form of potassium salt, which was dissolved in warm water and acidified by acetic acid to precipitate the product, and the obtained solid was recrystallized from ethanol.

Reddish brown; Yield: 96%; mp 290–292 °C; IR (V_{\max} , cm^{-1}): 1489 (C=S), 1715 and 1772 (3C=O), 3100–3400 (2NH, NH₂); ¹H NMR (δ , DMSO d_6): 1.31 (t, $J = 7.2$ Hz, 3H, CH₃), 4.24 (q, $J = 7.2$ Hz, 2H, CH₂), 7.01–8.02 (m, 6H, ArH, NH₂), 12.76 (s, 2H, 2NH). ¹³CNMR (DMSO d_6): 14.89 (CH₃), 62.07 (CH₂), 125.05, 126.04, 133.13, 141.12, 145.59 (Ar-C), 168.04 (C = S), 164.22, 165.08, 166.25 (3C = O) ppm; DEPT-135 δ (ppm) 21.99(CH₃), 60.57(CH₂), 123.21 (CH), 123.46(CH), 123.58 (CH), 123.65 (CH); Analysis calculated for C₁₅H₁₃N₃O₄S (331.35); C, 54.37; H, 3.95; N, 12.68; S, 9.68; Found; C, 54.41; H, 3.98; N, 12.72; S, 9.74. MS (m/z): 331.35: [M⁺].

2.1.2. General procedure of compound 2a, b

A mixture of compound **1** (1.0 mmol), urea and / or thiourea (1.0 mmol), trimethylamine (few drops), and ethanol (20.0 mL) was subjected to microwave irradiation for about 20 min. After the reaction was completed (TLC), the mixture was concentrated and the obtained solid was collected by filtration and recrystallized from ethanol to provide **2a, b**.

2.1.2.1. 2'-Thioxo-2',3'-dihydro-1'H-spiro[indene-2,4'-pyrimido[4,5-d]pyrimidine]-1,3, 5',7'(6'H,8'H)-tetraone (2a). Red; Yield: 95%; mp 235–237 °C; IR (V_{\max} , cm^{-1}), 1476 (C=S), 1675 (C=O), 3100–3400 (3NH); ¹H NMR (δ , DMSO d_6): 7.01–8.02 (m, 4H, ArH), 10.55 (s, 1H, NH), 11.38 (s, 1H, NH), 11.99 (s, 1H, NH), 12.27 (s, 2H, NH); ¹³CNMR (DMSO d_6): 120.0, 128.25, 131.13, 141.12, 161.07 (Ar-C), 170.04 (C=S), 162.14, 163.28, 195.25 (3C=O) ppm. Analysis calculated for C₁₄H₈N₄O₄S (328.30); C, 51.22; H, 2.46; N, 17.07; S, 9.77; Found; C, 51.26; H, 2.51; N, 17.13; S, 9.82. MS (m/z): 328.30: [M⁺].

2.1.2.2. 2',7-dithioxo-2',3',7',8'-tetrahydro-1'H-spiro[indene-2,4'-pyrimido[4,5-d]pyrimidine]-1,3,5'(6'H)-trione (2b). Reddish brown; yield: 97%; mp 260–262 °C; IR (V_{\max} , cm^{-1}): 1491 (C=S), 1667 (C=O), 3100–3400 (4NH); ¹H NMR (δ , DMSO d_6): 7.22–7.91 (m, 4H, ArH), 9.79 (s, 1H, NH), 10.28 (s, 1H, NH), 11.81 (s, 1H, NH), 12.25 (s, 1H, NH). ¹³CNMR (DMSO d_6): 120.55, 126.04, 133.13, 141.12, 161.07 (Ar-C), 165.36, 185.78 (C=O), 169.03, 170.04, (C=S) ppm; analysis calculated for C₁₄H₈N₄O₃S₂ (344.37); C, 48.83; H, 2.34; N, 16.27; S, 18.62; Found; C, 48.86; H, 2.39; N, 16.31; S, 18.66. MS (m/z): 344.37: [M⁺].

2.1.3. 7'-Thioxo-7',8'-dihydrospiro[indene-2,5'-pyrimido[4,5-d][1,3]oxazine]-1,3,4'(6'H)-trione (3)

A mixture of compound (**1**) with equimolecular amount of formic acid was refluxed for 10 h. The solid product was collected and recrystallized from ethanol to provide (**3**).

Pale yellow; Yield: 69%; m.p. 276–278 °C; IR (V_{\max} , cm^{-1}): 1240 (C=S), 1654, 1707 (3C=O); 3100–3400 (2NH); ¹H NMR (δ , DMSO d_6): 7.50–8.00 (m, 5H, ArH), 10.35 (s, 1H,

NH), 11.67 (s, 1H, NH); ¹³CNMR (DMSO d_6): 129.16, 130.79, 133.86, 134.05, 135.16, 137.28, 140.57, 141.71 (Ar-C), 163.05 (CH=N), 163.25, 196.58 (3C=O), 180.56 (C=S) ppm. Analysis calculated for C₁₄H₇N₃O₄S (313.29); C, 53.67; H, 2.25; N, 13.41; S, 10.23; Found; C, 53.69; H, 2.27; N, 13.46; S, 10.28. MS (m/z): 313.29 [M⁺].

2.1.4. Synthesis of Schiff base (4a, b)

Equimolar concentrations of compound **1** (1.0 mmol) and different aryl aldehydes (1.0 mmol) were stirred for 6–8 h at room temperature using ethanol (20.0 mL) and then 2–3 drops of glacial acetic acid were added to the mixture. The progress of the reaction was followed by TLC until the reaction was complete. It was cooled to 0 °C, the precipitate was filtered, washed with diethyl ether and the residue was recrystallized from ethanol to give the corresponding (**4a, b**).

2.1.4.1. Ethyl 6'-(4-hydroxy-2-nitrobenzylidene)amino)-1,3-dioxo-2'-thioxo-1,2',3,3'-tetrahydro-1'H-spiro[indene-2,4'-pyrimidine]-5'-carboxylate (4a). Orange; Yield: 76%; m.p. 231–232; IR (V_{\max} , cm^{-1}): 1250 (C=S), 1685, 1712 (C=O), 3100–3400 (2NH); ¹H NMR (δ , DMSO d_6): 1.62 (t, 3H, CH₃), 4.55 (q, 2H, CH₂), 6.86–8.20 (m, 7H, ArH), 8.61 (s, 1H, HC=N), 10.27 (s, 1H, NH), 11.28 (s, 1H, NH), 11.96 (s, 1H, OH); ¹³CNMR (DMSO d_6): 10.9 (CH₃), 57.82 (O—CH₂—), 95.26 (O=C—C—C=O), 85.68, 162.82, 115.16, 122.79, 125.86, 133.05, 131.16, 143.57, 141.28, 158.71 (Ar-C), 163.05 (CH=N), 163.25, 196.58 (3C=O), 180.56 (C=S) ppm. Analysis calculated for C₂₂H₁₆N₄O₇S (480.45); C, 55.00; H, 3.36; N, 11.66; S, 6.67; Found; C, 55.07; H, 3.39; N, 11.67; S, 6.71. MS (m/z): 480.45 [M⁺].

2.1.4.2. Ethyl 6'-(4-hydroxybenzylideneamino)-1,3-dioxo-2'-thioxo-1,2',3,3'-tetrahydro-1'H-spiro [indene-2, 4'-pyrimidine]-5'-carboxylate (4b). Red; Yield: 82%; m.p. 215–218; IR (V_{\max} , cm^{-1}): 1237 (C=S), 1712 (C=O), 2942 (Ar-H), 3100–3400 (2NH); ¹H NMR (δ , DMSO d_6): 1.29 (t, $J = 6.9$ Hz, 3H, CH₃), 4.55 (q, $J = 6.9$ Hz, 2H, O—CH₂—), 7.01–8.02 (m, 9H, ArH), 10.48 (s, H, 2NH); ¹³CNMR (DMSO d_6): 15.9 (CH₃), 62.5 (O—CH₂—), 95.26 (O=C—C—C=O), 85.68, 115.16, 122.79, 125.86, 131.16, 143.57, 141.28, 158.71, 162.82, (Ar-C), 163.05 (CH=N), 163.25, 196.58 (2C=O), 180.56 (C=S) ppm. Analysis calculated for C₂₂H₁₇N₃O₄S (419.45); Calcd, C, 63.00; H, 4.09; N, 10.02; S, 7.64; Found; C, 63.05; H, 4.12; N, 10.7; S, 7.69. MS (m/z): 419.45 [M⁺].

2.1.5. General procedure for synthesis of compounds (5a-e):

A mixture of compound **1** (1.0 mmol) and equivalent amount of *p*-substituted aniline (*p*-nitroaniline, *p*-methoxy aniline, *p*-methylaniline, aniline) and or 2-amino pyridine (1.0 mmol) and excess of formaldehyde (37%) in acetonitrile at room temperature was stirred for 4 h. The solid formed was collected and crystallized from ethanol to provide (**5a-e**) in good yield.

2.1.5.1. Synthesis of 6'-(4-nitrophenyl)-2'-thioxo-2',3',7',8'-tetrahydro-1'H-spiro[indene-2,4'-pyrimido[4,5-d]pyrimidine]-1,3,5'(6'H)-trione (5a). Yellow; Yield: 95%; m.p. 232–234 °C; IR (V_{\max} , cm^{-1}): 1245 (C=S), 1710 and 1597 (3C=O), 3100–3400 (3NH); ¹H NMR (δ , DMSO d_6): 4.81 (s, 2H, CH₂), 7.01–8.02 (m, 8H, ArH), 10.25 (s, 2H, 2NH), 10.56 (s, 1H, NH); ¹³C-

CNMR (DMSO d_6): 58.22 (CH₂), 116.88, 117.58, 118.66, 119.86, 120.01, 123.27, 124.50, 125.45, 126.23, 141.71 (Ar-C), 153.93, 156.45, 160.89 (3C=O), 162.77 (C=S) ppm. Analysis calculated for C₂₀H₁₃N₅O₅S (435.41); C, 55.17; H, 3.01; N, 16.08; S, 7.36; Found; C, 55.21; H, 3.15; N, 16.13; S, 7.41. MS (m/z): 435.41 [M⁺].

2.1.5.2. *6'-(4-methoxyphenyl)-2'-thioxo-2',3',7',8'-tetrahydro-1'H-spiro[indene-2,4'-pyrimido[4,5-d]pyrimidine]-1,3,5'(6'H)-trione (5b)*. Brown; Yield: 76%; m.p. 261–262 °C; Yield: 76%; m.p. 261–262 °C; IR (V_{\max} , cm⁻¹): 1461(C=S), 1672 (C=O), 3100–3400 (3NH); ¹H NMR (δ , DMSO d_6): 3.89 (s, 3H, CH₃) 4.85 (s, 2H, CH₂), 6.69–8.01 (m, 8H, ArH), 10.28 (s, 2H, 2NH), 11.17 (s, 1H, NH); ¹³CNMR (DMSO d_6): 15.07 (CH₃), 63.05 (CH₂), 95.26 (O=C–C–O), 162.82, 116.16, 117.79, 118.86, 131.16, 133.05, 140.28, 141.57, 142.71 (Ar-C), 158.79, 160.13, 161.42 (C=O), 163.90 (C=S) ppm. Analysis calculated for C₂₁H₁₆N₄O₄S (420.44); C, 59.99; H, 3.84; N, 13.33; S, 7.63; Found; C, 60.03; H, 3.87; N, 13.37; S, 7.68. MS (m/z): 420.44 [M⁺].

2.1.5.3. *2'-Thioxo-6'-(p-tolyl)-2',3',7',8'-tetrahydro-1'H-spiro[indene-2,4'-pyrimido[4,5-d]pyrimidine]-1,3,5'(6'H)-trione (5c)*. Green; Yield: 70%; m.p. 242–244 °C; IR (V_{\max} , cm⁻¹): 1354 (C=S), 1678 (C=O), 3100–3400 (3NH); ¹H NMR (δ , DMSO d_6): 2.81 (s, 3H, CH₃), 4.75 (s, 2H, CH₂), 6.86–8.69 (m, 8H, ArH), 11.25 (s, 2H, 2NH), 11.87 (s, 1H, NH); ¹³CNMR (DMSO d_6): 21.25 (CH₃), 63.05 (CH₂), 95.26 (O=C–C–O), 85.68, 162.82, 117.16, 118.79, 119.86, 120.16, 129.75, 141.28, 143.57, 158.71 (Ar-C), 163.25, 196.58 (C=O), 180.56 (C=S) ppm. Analysis calculated for: C₂₁H₁₆N₄O₃S (404.44); C, 62.36; H, 3.99; N, 13.85; S, 7.93; Found; C, 62.39; H, 4.02; N, 13.86; S, 7.97. MS (m/z): 404.44 [M⁺].

2.1.5.4. *6'-Phenyl-2'-thioxo-2',3',7',8'-tetrahydro-1'H-spiro[indene-2,4'-pyrimido[4,5-d]pyrimidine]-1,3,5'(6'H)-trione (5d)*. Red; Yield: 72%; m.p. 217–219 °C; IR (V_{\max} , cm⁻¹): 1246 (C=S), 1654, 1716 (3C=O), 3100–3400 (3NH); ¹H NMR (δ , DMSO d_6): 5.19 (s, 2H, CH₂), 7.01–8.02 (m, 9H, ArH), 12.19 (s, 3H, 3NH); ¹³CNMR (DMSO d_6): 62.70 (CH₂), 112.17, 122.28, 125.22, 128.33, 130.46, 141.26, 143.57, 158.71 (Ar-C), 162.12, 185.01 (C=O), 158.65 (C=S) ppm; DEPT135 spectrum (ppm): 62.70 (CH₂), 122.28, 123.35, 125.22, 128.33 (Ar-); Analysis calculated for C₂₁H₁₆N₄O₃S (390.42); C, 61.53; H, 3.61; N, 14.35; S, 8.21; Found; C, 61.56; H, 3.63; N, 14.38; S, 8.26. MS (m/z): 390.42 [M⁺].

2.1.5.5. *Synthesis of 6'-(pyridin-2-yl)-2'-thioxo-2',3',7',8'-tetrahydro-1'H-spiro[indene-2,4'-pyrimido[4,5-d]pyrimidine]-1,3,5'(6'H)-trione (5e)*. Reddish brown; Yield: 69%; m.p. 252–253 °C; IR (V_{\max} , cm⁻¹): 1247(C=S), 1654, 1720 (3C=O); 3100–3400 (3NH); ¹H NMR (δ , DMSO d_6): 5.28 (s, 2H, CH₂), 7.01–8.02 (m, 8H, ArH), 10.26 (s, 2H, 2NH), 11.59 (s, 1H, NH); ¹³CNMR (DMSO d_6): 56.32 (CH₂), 95.26 (O=C–C–O), 85.68, 112.48, 122.79, 125.86, 131.16, 133.05, 137.38, 139.10, 142.06, 147.94, 158.71 (Ar-C), 163.25 (C=O), 196.58 (2C=O), 180.56 (C=S) ppm. Analysis calculated for C₁₉H₁₃N₅O₃S (391.40); C, 58.30; H, 3.35; N, 17.89; S, 8.19; Found; C, 58.36; H, 3.41; N, 17.93; S, 8.23. MS (m/z): 391.40 [M⁺].

2.1.6. *Synthesis of 6'-amino-1,3-dioxo-2'-thioxo-1,2',3,3'-tetrahydro-1'H-spiro[indene-2,4'-pyrimidine]-5'-carbohydrazide (7)*

A mixture of compound **1** (1.0 mmol) and hydrazine hydrate (3.0 mL) in 30.0 mL EtOH was refluxed for 5 h and / or subjected to microwave for ten minutes. Then, the reaction mixture was concentrated under reduced pressure, and the residue washed with acidified cold H₂O and then triturated with MeOH. The formed orange product was filtered off, washed well with MeOH, and recrystallized from ethanol solvent to afford the hydrazinyl derivatives **7**.

Orange; Yield: 90%; mp 248–250 °C; IR (V_{\max} , cm⁻¹): 1484 (C=S), 1652 (C=O), 3100–3400 (3NH, 2NH₂); ¹H NMR (δ , DMSO d_6): 6.30–8.45 (m, 8H, for ArH and 2NH₂), 10.19 (s, 1H, NH), 10.33(s, 2H, 2NH); ¹³CNMR (DMSO d_6): 125.05, 126.04, 133.13, 141.12, 145.59 (Ar-C), 168.04 (C=S), 165.08, 167.02 (C=O) ppm. Analysis calculated for: C₁₃H₁₁N₅O₃S (317.32); C, 49.21; H, 3.49; N, 22.07; S, 10.10; Found; C, 49.26; H, 3.53; N, 22.13; S, 10.15. MS (m/z): 317.32[M⁺].

2.1.6.1. *Synthesis of 6'-amino-5'-(5-hydroxy-3-methyl-1H-pyrazole-1-carbonyl)-2'-thioxo-2',3'-dihydro-1'H-spiro[indene-2,4'-pyrimidine]-1,3-dione (8)*. A mixture of compound (**7**) (1.0 mmol) and ethyl acetoacetate (1.0 mmol) in ethanol (20.0 mL) and three drops of glacial acetic acid the reaction mixture was subjected to microwave for about 10 min. The reaction mixture was allowed to cool at room temperature and then poured into crushed-ice. The separated solid was filtered off, dried and crystallized from EtOH/DMF (2:1) to give compound **8**.

Light brown; Yield: 98%; m.p.: 190–192 °C; IR (V_{\max} , cm⁻¹): 1271(C=S), 1616 (C=O), 3100–3400 (2NH, NH₂), 3590 (OH); ¹H NMR (δ , DMSO d_6): 1.21 (s, 3H, CH₃), 6.32 (s, 1H, pyrazole H), 7.50–8.00 (m, 4H, ArH), 10.27 (s, 2H, NH₂), 11.12 (s, 2H, 2NH), 12.41 (s, 1H, OH); ¹³CNMR (DMSO d_6): 15.02 (CH₃), 92.88, 115.29, 120.04, 125.23, 129.67, 141.12, 153.02, 180.59 (Ar-C), 163.52, 163.89, 165.85 (3C=O), 177.36 ppm (C=S) ppm. Analysis calculated for C₁₇H₁₃N₅O₄S (383.38); C, 53.26; H, 3.42; N, 18.27; S, 8.36; Found; C, 53.31; H, 3.46; N, 18.30; S, 8.39. MS (m/z): 383.38 [M⁺].

2.1.6.2. *Synthesis of 6'-amino-5'-(3-amino-5-hydroxy-1H-pyrazole-1-carbonyl)-2'-thioxo-2',3'-dihydro-1'H-spiro[indene-2,4'-pyrimidine]-1,3-dione (9)*. A mixture of compound (**7**) (1.0 mmol) and ethyl cyanoacetate (1.0 mmol) in ethanol (20.0 mL) and three drops of glacial acetic acid was subjected to microwave for about 10 min. After cooling, the reaction mixture was poured into crushed-ice, and the Separated solid was filtered off, dried well and crystallized from acetic acid to afford compound **9**.

Orange; Yield 96%; m.p.: 225–227 °C; IR (V_{\max} , cm⁻¹): 1245 (C=S), 1624 (C=O), 3100–3400 (2NH, 2NH₂), 3596 (OH), ¹H NMR (δ , DMSO d_6): 6.11 (s, 1H, pyrazole H), 6.52 (s, 2H, NH₂), 7.50–8.00 (m, 4H, ArH), 10.27 (s, 2H, NH₂), 11.12 (s, 2H, 2NH), 12.53 (s, 1H, OH); ¹³CNMR (DMSO d_6): 118.88, 119.29, 120.04, 125.23, 129.67, 133.13, 137.12, 138.02, 142.59 (Ar-C), 163.52, 163.89, 165.85 (3C=O); 177.36 (C=S) ppm. Analysis calculated for C₁₆H₁₂N₆O₄S (384.37); C, 50.00; H, 3.15; N, 21.86; S, 8.34; Found; C, 50.14; H, 3.20; N, 21.89; S, 8.39. MS (m/z): 384.37 [M⁺].

2.1.6.3. *Synthesis of 6'-amino-5'-(3,5-dihydroxy-1H-pyrazole-1-carbonyl)-2'-thioxo-2',3'-dihydro-1'H-spiro[indene-2,4'-pyrimidine]-1,3-dione (10)*. A mixture of (**7**) (1.0 mmol) and diethyl malonate (1.0 mmol) in ethanol (20.0 mL) and three drops of glacial acetic acid was subjected to microwave for about 10 min. After cooling, the reaction mixture was poured into crushed-ice and the separated solid was filtered off, dried well and crystallized from EtOH/ DMF (2:1) to give compound **10**.

Brown; Yield: 99%; m.p. 206–208 °C; IR (V_{\max} , cm^{-1}): 1489 (C=S), 1716, (C=O), 3100–3400 (2NH, NH₂), 3596 (2OH); ¹H NMR (δ , DMSO d_6): 6.00 (s, 1H, pyrazole proton), 7.01–8.02 (m, 4H, ArH), 10.29 (s, 2H, NH₂), 11.98 (s, 2H, 2NH), 12.16 (s, 2H, 2OH); ¹³CNMR (DMSO d_6): 120.04, 123.13, 126.12, 128.11, 34.84, 135.79, 141.12, 145.02 (Ar-C), 168.04 (C=S), 167.78, 171.56, (2C=O) ppm. Analysis calculated for: C₁₆H₁₁N₅O₅S (385.35); C, 49.87; H, 2.88; N, 18.17; S, 8.32; Found; C, 49.89; H, 2.91; N, 18.22; S, 8.36; MS (m/z): 385.35 [M⁺].

2.1.7. Synthesis of compound (11)

Compound (**11**) was prepared according to the reported method Reddy, 1986.

Green method for preparation of (11)

A Mixture of 1, 2, 3-indenetrione (1.0 mmol) and thiosemicarbazide (1.0 mmol) in water was stirred at room temperature (23 °C) using ultrasonic irradiation for 7 min to provide the corresponding (**11**) in 99% yield.

2.1.7.1. *N-(3'-acetyl-1,3-dioxo-1,3-dihydro-3'H-spiro[indene-2,2'-[1,3,4]thiadiazol]-5'-yl)acetamide (12)*. A mixture of thiosemicarbazone derivative (**11**, 1.0 mmol) and acetic anhydride was subjected to microwave irradiation for 10 min at 50 °C to provide the corresponding (**12**)

Reddish brown; Yield: 99%, m.p. 220–222 °C; IR (V_{\max} , cm^{-1}): 1665, 1716 (4C=O), 2970 (Ar-H), 3074 (NH), ¹H NMR (δ , DMSO d_6): 1.33 (s, 3H, CH₃), 2.0 (s, 3H, CH₃), 7.01–8.02 (m, 4H, ArH), 10.58 (s, 1H, NH); ¹³CNMR (DMSO d_6): 120.01, 139.15, 140.03, 141.06, 142.21 (Ar-C), 161.03, 183.42, (2C=O), 184.27 (C=O) ppm. Analysis calculated for: C₁₄H₁₁N₃O₄S (317.32); C, 52.99; H, 3.49; N, 13.24; S, 10.10; Found; C, 53.03; H, 3.53; N, 13.26; S, 10.14; MS (m/z): 317.32 [M⁺].

2.1.8. General synthesis of compounds (13a-d)

A mixture of compound **12** (1.0 mmol), the appropriate aromatic aldehyde (1.0 mmol), NaOH 40% and solvent were taken in a beaker and sonicated for 15–30 min in the water bath of an ultrasonic cleaner bath. The progress of the reaction was monitored by TLC. The reaction mixture was then cooled in ice-water bath. The formed precipitate was filtered, washed with cool water, dried and recrystallized from alcohol to afford chalcones (**13a-d**).

2.1.8.1. *N-(1,3-dioxo-3'-(3-phenylacryloyl)-1,3-dihydro-3'H-spiro[indene-2,2'-[1,3,4]thiadiazol]-5'-yl)acetamide (13a)*. Pale Yellow ;Yield :96%; m.p. 240–242 °C; IR (V_{\max} , cm^{-1}): 1600 (C=C), 1683 (C=O), 2981 (Ar-H), 3070 (NH); ¹H NMR (δ , DMSO d_6): 1.29 (s, 3H, CH₃), 7.05–7.61 (m, 4H, ArH), 7.65 (d, $J = 15.63$ Hz, 1H, H) 7.65–7.72 (m, 3H, ArH), 7.76 (d, $J = 15.61$ Hz, 1H, H), 8.02 (d, $J = 9.11$ Hz,

2H, ArH); 10.23 (s, 1H, NH); ¹³CNMR (DMSO d_6): 126.23, 127.14, 128.15, 129.27, 130.12, 131.06, 133.02, 134.14 (Ar-C), 165.13 (C=O) ppm. Analysis calculated for C₂₁H₁₅N₃O₄S (405.43); C, 62.21; H, 3.73; N, 10.36; S, 7.91; Found; C, 62.25; H, 3.79; N, 10.39; S, 7.95; MS (m/z): 405.43 [M⁺].

2.1.8.2. *N-(3'-(3-(4-hydroxy-2-nitrophenyl)acryloyl)-1,3-dioxo-1,3-dihydro-3'H-spiro [indene -2,2'-[1,3,4]thiadiazol]-5'-yl)acetamide (13b)*. Yellow; Yield: 93%, m.p. 252–254 °C; IR (V_{\max} , cm^{-1}): 1600 (C=C), 1683, 1716 (C=O), 2972 (Ar-H), 3100–3400 (NH); ¹H NMR (δ , DMSO d_6): 2.31 (s, 3H, CH₃), 7.06–7.12 (m, 4H, ArH), 7.64 (d, $J = 15.57$ Hz, 1H, H), 7.75 (d, $J = 15.63$ Hz, 1H, H), 8.02–8.16 (m, 3H, ArH), 10.21 (s, 1H, NH), 12.13(s, 1H, OH); ¹³CNMR (DMSO d_6): 126.25, 127.17, 128.18, 129.29, 130.15, 131.12, 133.11, 134.18 (Ar-C), 165.26, (C=O) ppm, Analysis calculated for C₂₁H₁₄N₄O₇S (466.42); C, 54.08; H, 3.03; N, 12.01; S, 6.87; Found; C, 54.14; H, 3.16; N, 12.07; S, 6.89; MS (m/z): 466.42 [M⁺].

2.1.8.3. *N-(3'-(3-(4-(dimethylamino)phenyl)acryloyl)-1,3-dioxo-1,3-dihydro-3'H-spiro [indene-2,2'-[1,3,4]thiadiazol]-5'-yl)acetamide (13c)*. Orang ;Yield :95%; m.p. 236–238 °C; IR (V_{\max} , cm^{-1}): 1616 (C=C), 1639 (C=O), 3100–3400 (NH); ¹H NMR (δ , DMSO d_6): 1.22 (s, 3H, CH₃), 2.32 (s, 6H, 2CH₃), 7.05–7.38 (m, 4H, ArH), 7.63 (d, $J = 15.53$ Hz, 1H, H), 7.76 (d, $J = 15.62$ Hz, 1H, H), 7.81–8.02 (d, $J = 9.14$ Hz, 2H, ArH), 12.25 (s, 1H, NH); ¹³CNMR (DMSO d_6): 39.05 (CH₃), 40.03 (CH₃), 111.03, 125.25, 126.23, 129.27, 135.14, 136.16, 138.22, 139.24, 141.03 (Ar-C), 163.13, 164.23, 190.26, 195.08 (C=O) ppm. Analysis calculated for C₂₃H₂₀N₄O₄S (448.49); C, 61.59; H, 4.49; N, 12.49; S, 7.15; Found; C, 61.63; H, 4.52; N, 12.55; S, 7.19. MS (m/z): 448.49 [M⁺].

2.1.8.4. *N-(3'-(3-(2-hydroxy-4-methoxyphenyl)acryloyl)-1,3-dioxo-1,3-dihydro-3'H-spiro [indene-2,2'-[1,3,4]thiadiazol]-5'-yl)acetamide (13d)*. Yellowish; Yield: 94%; m.p. 263–265 °C; IR (V_{\max} , cm^{-1}): 1618 (C=C), 1638 (C=O), 3100–3400 (NH), 3551 (OH). ¹H NMR (δ , DMSO d_6): 1.03 (s, 3H, CH₃), 3.74 (s, 3H, OCH₃), 7.05–7.26 (m, 4H, ArH), 7.63 (d, $J = 15.53$ Hz, 1H, H), 7.76 (d, $J = 15.62$ Hz, 1H, H), 7.80–8.02 (m, 2H, ArH), 12.25 (s, 1H, NH). ¹³CNMR (DMSO d_6): 25.67, 39.05 (2CH₃), 111.03, 125.25, 126.23, 129.27, 135.14, 136.16, 138.22, 139.24, 141.03 (Ar-C), 163.13, 164.23, 190.26, 195.08 (C=O) ppm. Analysis calculated for: C₂₂H₁₇N₃O₆S (451.45); C, 58.53; H, 3.80; N, 9.31; S, 7.10; Found; C, 58.56; H, 3.85; N, 9.33; S, 7.16. MS (m/z): 451.45 [M⁺].

2.1.9. Synthesis of pyrazoles (15a, b)

A mixture of chalcones (**13a, b**) (1.0 mmol) and phenyl hydrazine (1.0 mmol) in ethanol was heated under reflux for 6 h and / or subjected to microwave for 10 min. The solvent was evaporated and the solid crystalized by diethyl ether to provide the corresponding pyrazoles (**15a, b**) in good yield.

2.1.9.1. *N-(3'-(1,5-diphenyl-4,5-dihydro-1H-pyrazol-4-yl)-1,3-dioxo-1,3-dihydro-3'H-spiro [indene-2,2'-[1,3,4]thiadiazol]-5'-yl)acetamide (15a)*. Brown ;Yield :88%; m.p: 270–272 °C; IR (V_{\max} , cm^{-1}): 1697, 1714 (C=O), 3100–3400 (NH); ¹H NMR (δ , DMSO d_6): 1.38(s,3H,CH₃),3.68(s,1H,CH₂),4.24(s,1H,

CH), 7.01–8.02 (m,15H,Ar-H,NH); ^{13}C NMR (DMSO d_6): 18.67 (CH₃), 55.66, 60.57 (CH,CH₂), 100.05, 121.12, 122.14, 125.03, 128.25, 129.21, 131.05 (Ar-C), 155.21, 165.03 (3C=O) ppm. Analysis calculated for C₂₇H₂₁N₃O₃S (495.55); C, 65.44; H, 4.27; N, 14.13; S, 6.47; Found; C, 65.45; H, 4.31; N, 14.15; S, 6.51. MS (m/z): 495.55 [M^+].

2.1.9.2. *N*-(3'-(5-(5-hydroxy-2-nitrophenyl)-1-phenyl-4,5-dihydro-1H-pyrazol-4-yl)-1,3-dioxo-1,3-dihydro-3'H-spiro[indene-2,2'-[1,3,4]thiadiazol]-5'-yl)acetamide (15b). Reddish-brown; Yield: 86%; m.p: 285–287 °C; IR (V_{max} , cm^{-1}): 1699, 1714 (C=O), 3100–3400 (NH). ^1H NMR (δ , DMSO d_6): 2.41 (s,3H,CH₃),3.68(s,1H,CH),4.92(s,1H,CH), 7.01–8.02(m,13H, Ar-H,NH), 12.35 (s,1H,OH); ^{13}C NMR (DMSO d_6): 21.64 (CH₃), 56.67(CH₂), 66.89(CH), 96.89, 121.51, 128.08, 128.88,128.27, 130.15,130.84,132.70, 136.06, 146.36, 147.32 (Ar-C), 155.66,161.65(3CO)ppm,Analysis calculated for C₂₇H₂₀N₆O₆S (556.55); C, 58.27; H, 3.62; N, 15.10; S, 5.76; Found; C, 58.29; H, 3.66; N, 15.14; S, 5.79 . MS (m/z): 556.55 [M^+].

2.2. Antifungal activity

2.2.1. Collection of samples

Tomato plants showing the damping-off disease symptoms were collected from tomato fields of Al-Jouf region. The infected plants were taken in plastic bags, transported to the laboratory for isolating the fungal causative agent of disease.

2.2.2. Isolation of fungi

basal portions of infected roots and stem were washed from the adhered soil and sterilized with NaClO₂ (2%) solution for 3 min, after that these parts were washed with sterile distilled H₂O for 30 min. By using Sterile forceps transferred pieces of 0.5 cm from each end of the roots to plates containing sterile Potato Dextrose Agar (PDA) medium with Rose Bengal (0.001 gm). Incubation was done at 27 °C ± 2 for 7 days [Ofunne, 1999](#).

2.2.3. Identification of fungi:

isolated fungi were identified based on microscopic and macroscopic characteristics [Rahjoo, 2008](#). Pathogenic fungi were additionally identified using molecular criteria according to sequence analysis of ITS1-5.8S rRNA-ITS2 region (Animal health research institute, Dokki, Giza, Egypt).

2.2.4. Effect of tested chemical compounds on the mycelial growth of *Fusarium oxysporum*:

Under sterile conditions, petri dish (9 cm diameter) was supplemented with sterilized PDA medium. A circular hole of 10 mm, 0.5 mm depth was made (using special instrument). Two hundred μl of each tested chemical compound (100 mg) which dissolved in 1.0 mL of DMSO was added into each well. Before adding the tested chemical solution, each Petri dish was inoculated with two discs of the tested fungus. Negative control was done using DMSO (100 μL) in well without chemicals, and positive control was done using Metalaxyl (100 μL). Incubation was performed at 27 °C for 6 days in the dark.

2.2.5. Determination of MIC

Diameter of inhibition zone (mm) around the well in different concentration (10, 15, 25, 50 and 100, mg/mL) of synthetic com-

pound was determined for measuring the antifungal activity. All tested compound were measured in triplicate and expressed as the average ± standard deviation of the measurements. Controls were done using DMSO without chemicals.

Inhibition percent (%) of fungal growth was calculated using the following formula [Hmouni et al., 1996](#):

$$\text{Percent of growth Inhibition (\%)} = \text{QUOTE } \frac{\text{DC} - \text{DT}}{\text{DC}} \times 100 \text{ QUOTE } \frac{\text{DC} - \text{DT}}{\text{DC}} \times 100 \frac{\text{C} - \text{F}}{\text{C}} \times 100$$

Where, C = Diameter of colony growth of the *Fusarium oxysporum* in control.

F = Diameter of colony growth of the *Fusarium oxysporum* in treated.

2.2.6. Microscopic analysis of the effect of tested chemical compounds on the mycelium growth

The microscopic images were taken at the faculty of Agriculture, Cairo University, using a SEM at 1000 and 3000 x. Samples were taken from mycelium treatment with tested chemical compounds at 25 mg/mL, then the mycelium was placed on a glass slide and using a metal coating equipment of samples (EDWARDS E306A), a copper bath was applied to the samples for 20 min for subsequent visualization. Finally, the general morphological and structural characteristics of the *F. oxysporum* mycelium were evaluated.

2.2.7. Testing the effect of chemical compounds on tomato seeds

2.2.7.1. *Agar plates*. One hundred ml of water agar (2%) with 10.0 mL of different chemical compounds (25.0 mg/mL) were poured each in conical flasks (250.0 mL) and then sterilized by autoclave. Tomato seeds were sterilized by 5% sodium hypochlorite solution for 5 min and then seeds were washed with sterilized distilled water for 30 min. Seeds were germinated for 2 days at 25 °C to select viable ones. Six Tomato seeds were planted in each flask with three discs of *F. oxysporum*. All flasks were incubated in a growth chamber at 25 °C with 12 h photoperiod. Experiments were performed with three replications were imposed on tomato seedling to record.

Percent germ ination (PG)

$$= \text{QUOTE } \frac{\text{number of seeds germ inated}}{\text{Total number of seeds sown}} \times 100$$

Percent disease incidence (PDI) = $\frac{\text{Numberofwiltedplants}}{\text{Totalnumberofplants}} \times 100$

2.2.8. Statistical analysis

The mean of analysis/determination results was formed by the statistical analysis by using ANOVA software. Statistical significance was defined as $P < 0.05$.

2.3. Docking study

In this study, we utilized MOE software Version 2008, Chemical Computing Group Inc, Montreal, Quebec, Canada) to do

this study (Bakr et al., 2021). Succinate dehydrogenase enzyme (SDH) with the cocrystallized ligand was downloaded from protein data bank (PDB: 2FBW). All the novel compounds were docked within the SDH enzyme. Binding energy scores and hydrogen bonds are listed within Table 6.

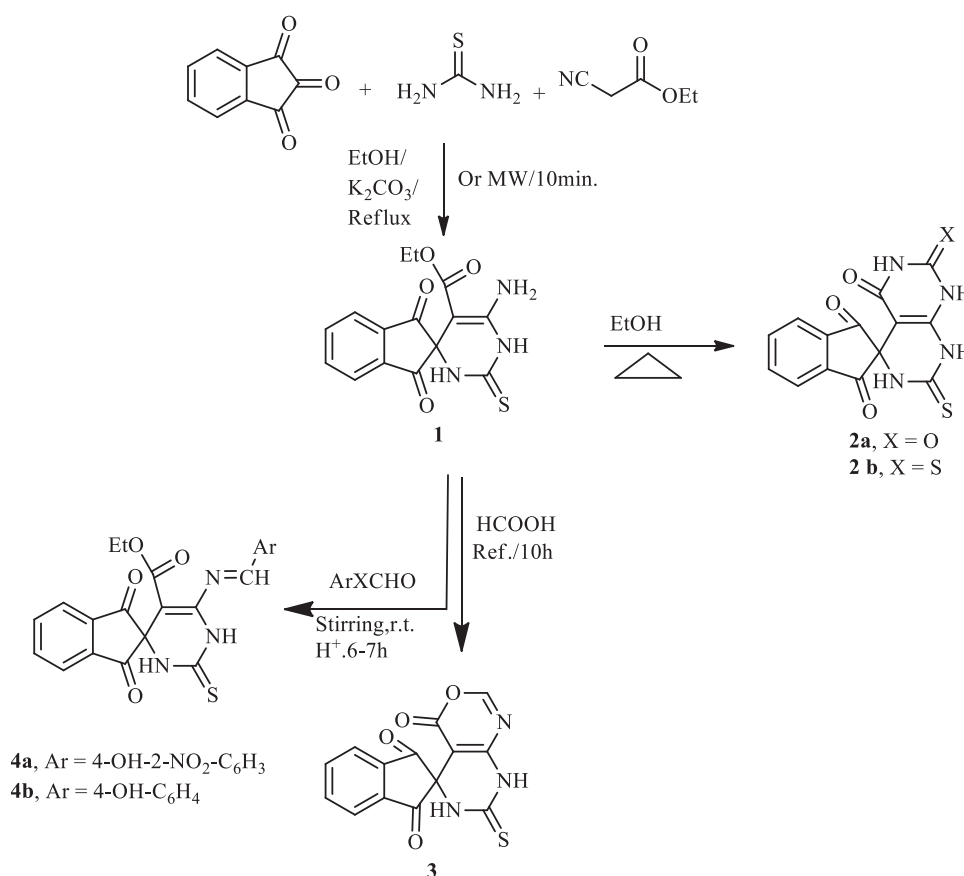
3. Results and discussion

3.1. Chemistry

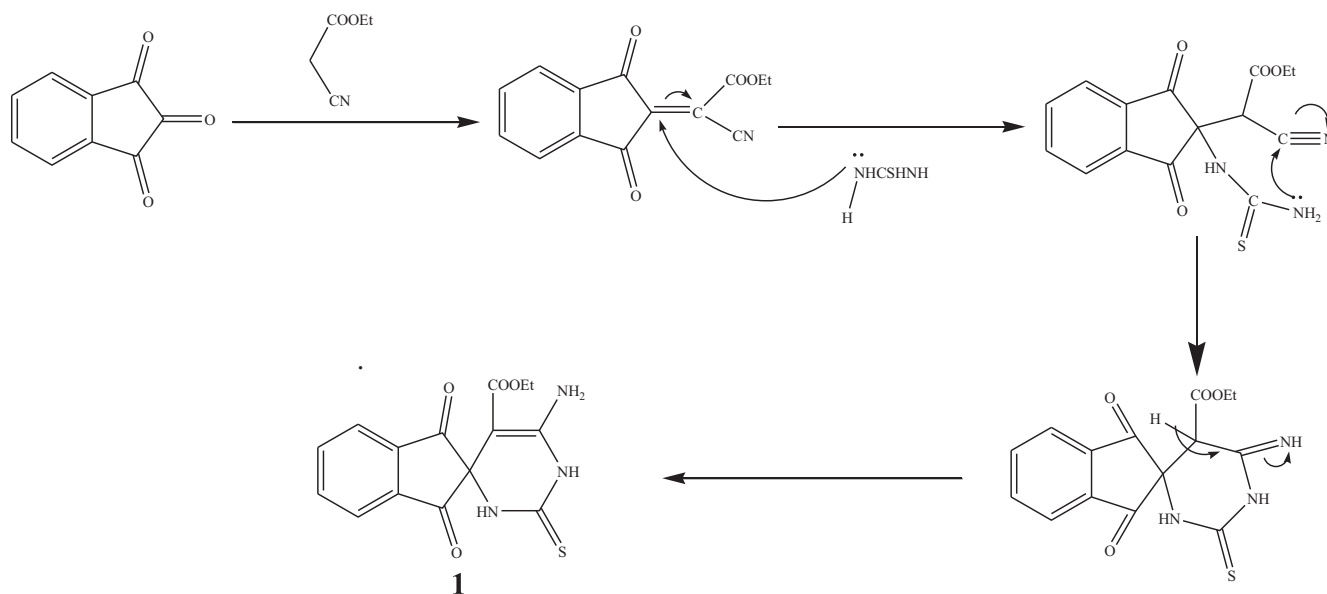
1, 2, 3-indenetrione, which contains three carbonyl groups, is a highly active electrophile. Initially, we tried to synthesize the spiro compound **1** via a cascade three-component protocol. The reaction was carried out by successive addition of reactants: 1, 2, 3-indenetrione, thiourea, and ethyl cyanoacetate in the existence of a catalytic portion of K_2CO_3 in a flask with ethanol at refluxed temperature (Scheme 1). TLC analysis showed that the reaction was achieved in 5 h to afford the target spiro compound **1** in 85% yield. To obtain the optimal reaction conditions, we investigated another energy source such as irradiation with microwave, which afforded a better yield (96%) in comparison to conventional conditions. To our delight, the Knoevenagel condensation product (Kundu and Pramanik, 2014) between 1,2,3-indenetrione and ethyl cyanoacetate did not observe in this cascade reaction and only a single product was detected spiro compound **1**. The molecular structure of the spiro compound **1** was interpreted from its

mass spectrometric analysis, FT-IR, 1H NMR, and ^{13}C NMR. The FT-IR spectrum of spiro compound **1** demonstrated wide absorption bands at $3100\text{--}3400\text{ cm}^{-1}$ attributed to the stretching frequencies of $(2NH, NH_2)$. Besides, the absorption bands at $1772, 1715, \text{ and } 1489\text{ cm}^{-1}$ are assigned to $C=O$ and $C=S$ groups. 1H NMR spectrum of spiro compound **1** exhibited a singlet signal that related to NH group at $\delta = 12.76$ ppm, one triplet signal is detected at $\delta = 1.31$ ppm for the methyl protons (CH_3), and one quartet at $\delta = 4.24$ ppm for the methylene protons (CH_2). Also, the multiples at $\delta = 7.01\text{--}8.02$ ppm were attributed to the aromatic protons and NH_2 proton. The existence of distinguished signals in the ^{13}C NMR spectrum of spiro compound **1** is compatible with the suggested structure. Moreover DEPT-135 δ (ppm) spectrum appeared negative signal in the opposite direction due to the CH_2 group at 60.57 ppm. The mass spectra agreement with the molecular structure of spiro compound **1**. The Suggested mechanism support the formation of spiro compound **1** was found in Scheme 2.

Treatment of the obtained ethyl spiro[indene-2,4'-pyrimidine]-5'-carboxylate **1** with urea and/or thiourea furnished the corresponding spiro[indene-2,4'-pyrimido[4,5-*d*]pyrimidine] derivatives **2a,b** in quantitative yields (Scheme 1). The structure of pyrimidine derivatives **2a, b** was established by IR, ^{13}C NMR, and mass spectra. The 7'-thioxo-7',8'-dihydro piro[indene-2,5'-pyrimido[4,5-*d*][1,3]oxazine]-1,3,4'(6'*H*)-trione **3** was constructed via the reaction of spiro compound **1** with



Scheme 1 Synthesis of indene-2,4'-pyrimidine-2-thione derivatives **1, 2a,b, 3,** and **4a,b.**



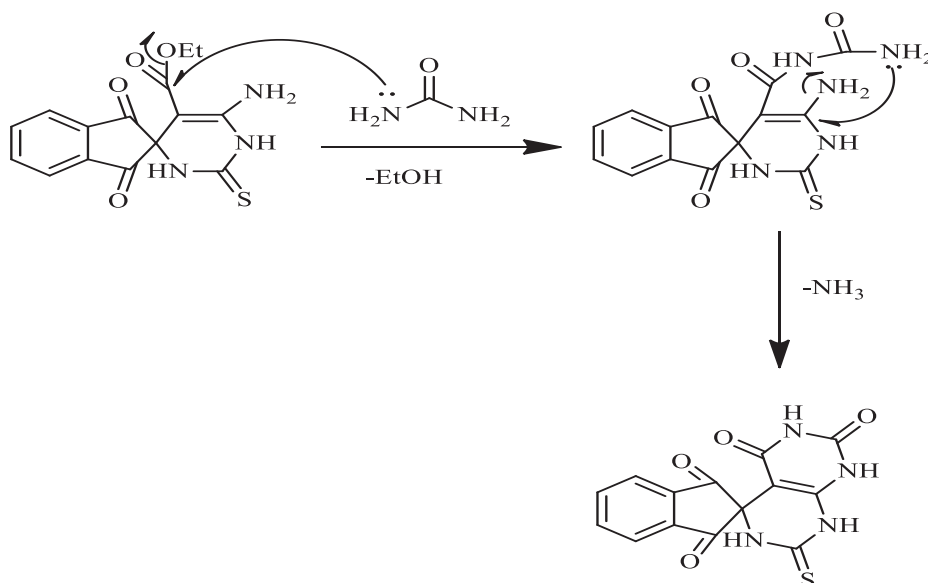
Scheme 2 A proposed mechanism for compound **1**.

formic acid. While the reaction of spiro compound **1** with two aromatic aldehydes (4-hydroxy-2-nitrobenzaldehyde and 4-hydroxybenzaldehyde) provided the appropriate Schiff bases **4a, b** in excellent yields (Scheme 1). FTIR, H-NMR, and mass spectra were utilized to establish the structure of obtained compounds **3** and **4a, b**. The IR spectrum of compound **3** indicated the existence of bands at 1654, 1707 and 1240 due to C=O and C=S, respectively. The ^{13}C NMR spectrum of compounds **3** revealed signals at 163.05, 163.25, 196.5 and 180.56 ppm for CH=N, C=O, and C=S groups, respectively. The mass spectrum indicated that the compound **3** has a molecule of water due to the presence of a peak at m/z 313 (see Scheme 3).

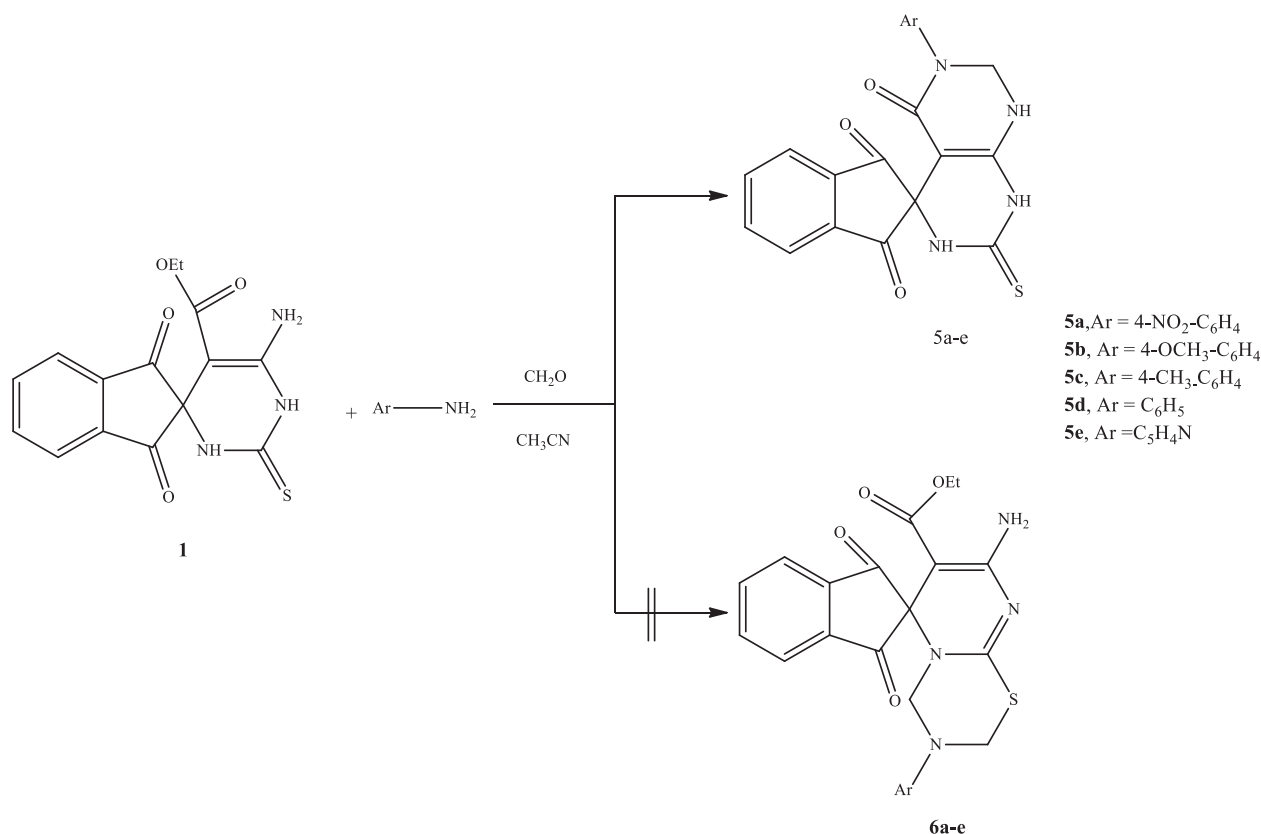
Treating the spiro compound (**1**) with one mole equivalent of *p*-substituted anilines and or 2-aminopyridine in excess of formaldehyde (37%) in acetonitrile at ambient temperature

could proceed to give the spiro[indene-2,4'-pyrimido[4,5-*d*]pyrimidine] (**5a-d**) or the other isomeric product spiro[indene-2,6'-pyrimido[2,1-*b*][1,3,5]thiadiazine] **6a-d** (Scheme 4). The TLC analysis revealed that the reaction produced only one product **5a-d** in high yield, and the other derivatives were undetectable (Scheme 4). The IR spectrum of the product **5a** as example is devoid of the C=O (ester) absorption peak, instead of showing the C=O (amide) peak at 1710 cm^{-1} . Moreover, the ^1H NMR spectrum of the compound **5a** was distinguished by the presence of one signal at $\delta = 4.81$ ppm, attributed to the methylene group (NCH₂N) besides the other protons at the anticipated chemical shifts. Also, the mass spectrum of the isolated compound **5a** revealed the required molecular ion peak.

On the other hand, the hydrazone derivative bearing pyrimidine-2-thiol core **7** was successfully synthesized utilizing



Scheme 3 A plausible mechanism for formation of compound **2a**.

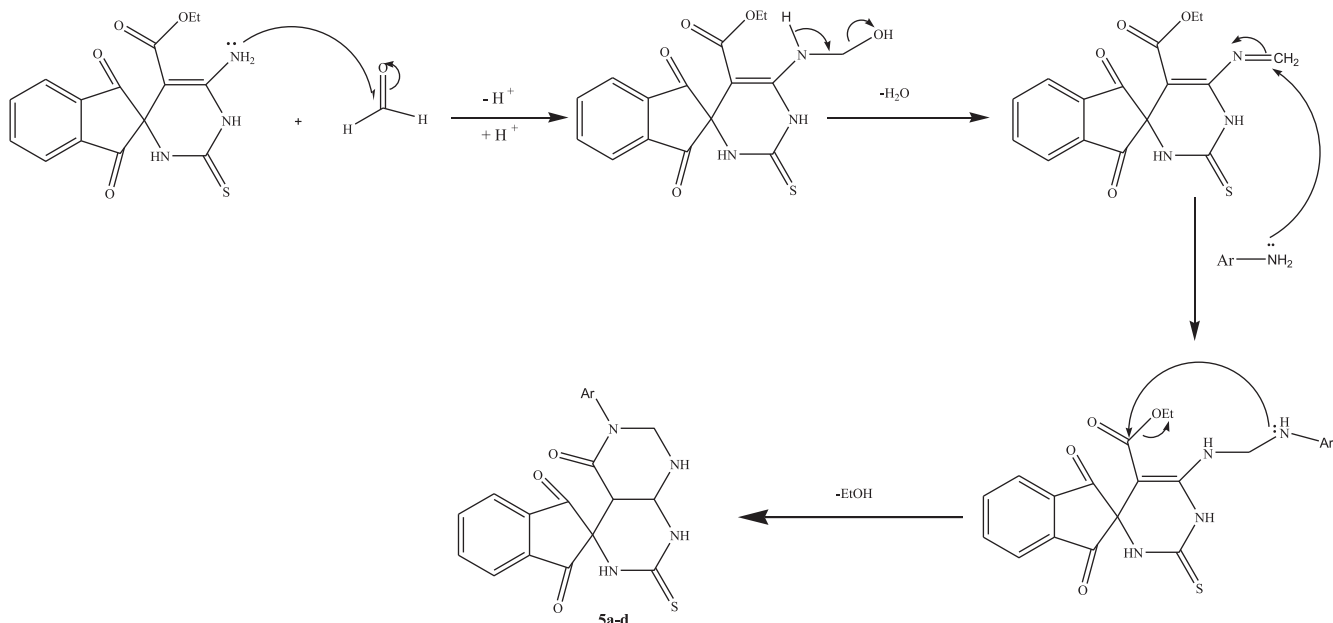


Scheme 4 Synthesis of derivative **5a-d**.

the microwave irradiation technique. Treatment of spiro compound **1** with hydrazine hydrate in ethanol produced the corresponding hydrazone **7** in an excellent yield (**Scheme 5**). IR spectra of hydrazone **7** revealed the existence of bands in the frequency of 1608, 3100–3400 cm⁻¹ corresponding to (C=O), (NH, NH₂), respectively, ¹HNMR spectra indicate

the absence of triplet and quartet peak for ethyl ester group, and its elemental analyses were aligned with the calculated values.

Reaction of hydrazone **7** and ethyl acetoacetate giving the pyrazole derivative **8** in moderate yield (78%, 8 h) under thermal conditions (**Scheme 6**). In an attempt to improve the reac-



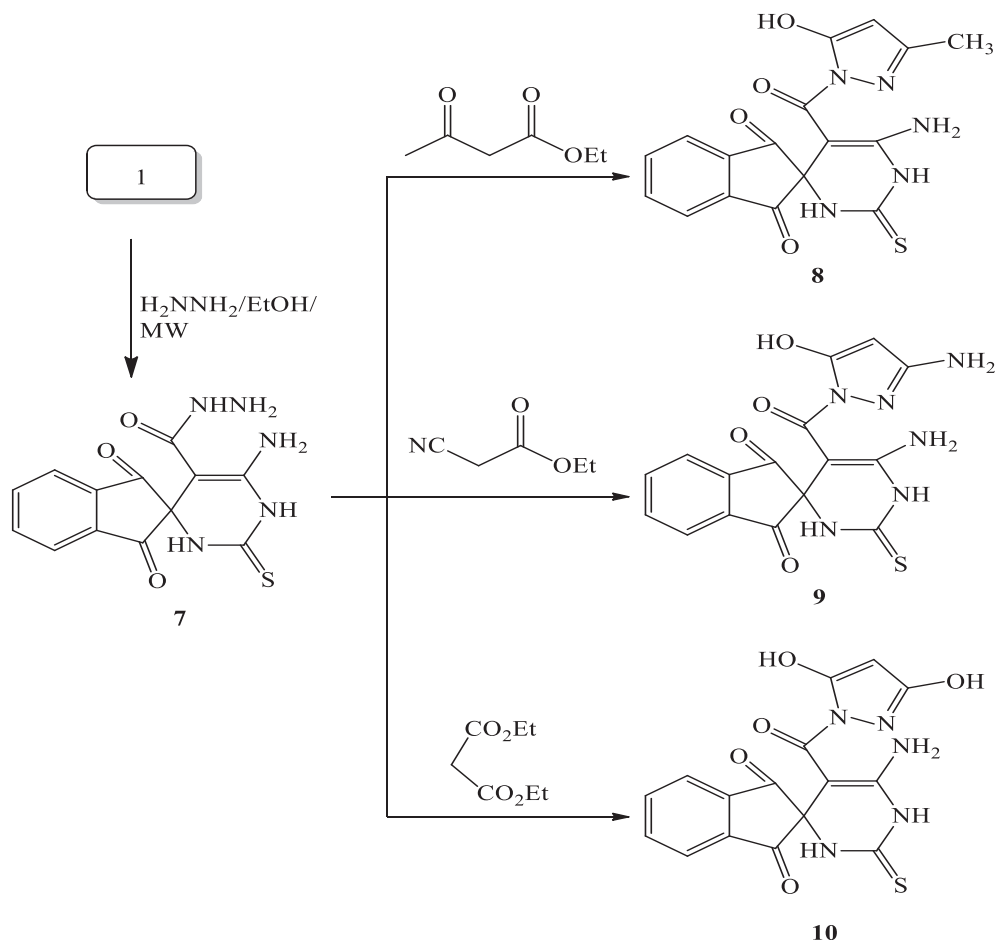
Scheme 5 A suggested mechanism for formation of compounds **5a-d**.

tion rate and yield, we used microwave irradiation as a sustainable energy source. Consequently, by conducting the aforementioned model reaction under microwave irradiation, both reaction rate and yield were highly improved; the desired product was obtained in 98% within 10 min. The optimistic results of the aforementioned model reaction (Scheme 6) prompted us to study the behaviors of the other active methylene derivatives (Scheme 6). Interestingly, the reaction of hydrazone **7** with ethyl cyanoacetate and / or diethylmalonate afforded the corresponding pyrazole derivatives **9**, **10** under microwave conditions in excellent yields (96 and 99%, respectively). The structure of compounds **8**, **9** and **10** was established by utilizing NMR, IR, and MS spectra. The IR spectrum of derivative **8** displayed a characteristic band at 1616 cm^{-1} , which was assigned to the carbonyl ($\text{C}=\text{O}$) stretching frequencies. The ^1H NMR spectrum of **8** exhibited one singlet signal at 6.32 ppm which was assigned to the pyrazole-4-proton. These results were supported further by the MS spectrum, which displayed the molecular ion peak at m/z 383 in agreement with the molar mass of the proposed structure.

From an industrial standpoint; we carried out a gram-scale assembly of pyrazole derivatives **8** under the optimal condition. Thus, irradiation of **7**, and ethyl acetoacetate in ethanol (**Scheme 5**) for 10 min (TLC) afforded the desired product **8** in super yield (98%). As the result, the current protocol could be employed as a distinguished protocol for the manufacturing

design of such pyrazole derivatives. Further, to assess the aforesaid protocol (Scheme 6) on the “greenness” scale, several green parameters including, yield economy, process mass intensity, reaction mass efficiency, E-factor, atom economy, and carbon efficiency (CE), and have been investigated (Tobiszewski et al., 2015). The elevated value of ecological-harmonious criteria, such as Yield Economy (9.80), Carbon efficiency (89.47%), Atom Economy (85.68%), and Reaction Mass Efficiency (83.96%) besides the low values of Process Mass Intensity (1.19) and E-factor (0.02) make the investigated microwave-assisted protocol ideal sustainable green process for construction of pyrazole vs. the conventional (thermal) process when comparable reaction chemistries are applied (Table 1).

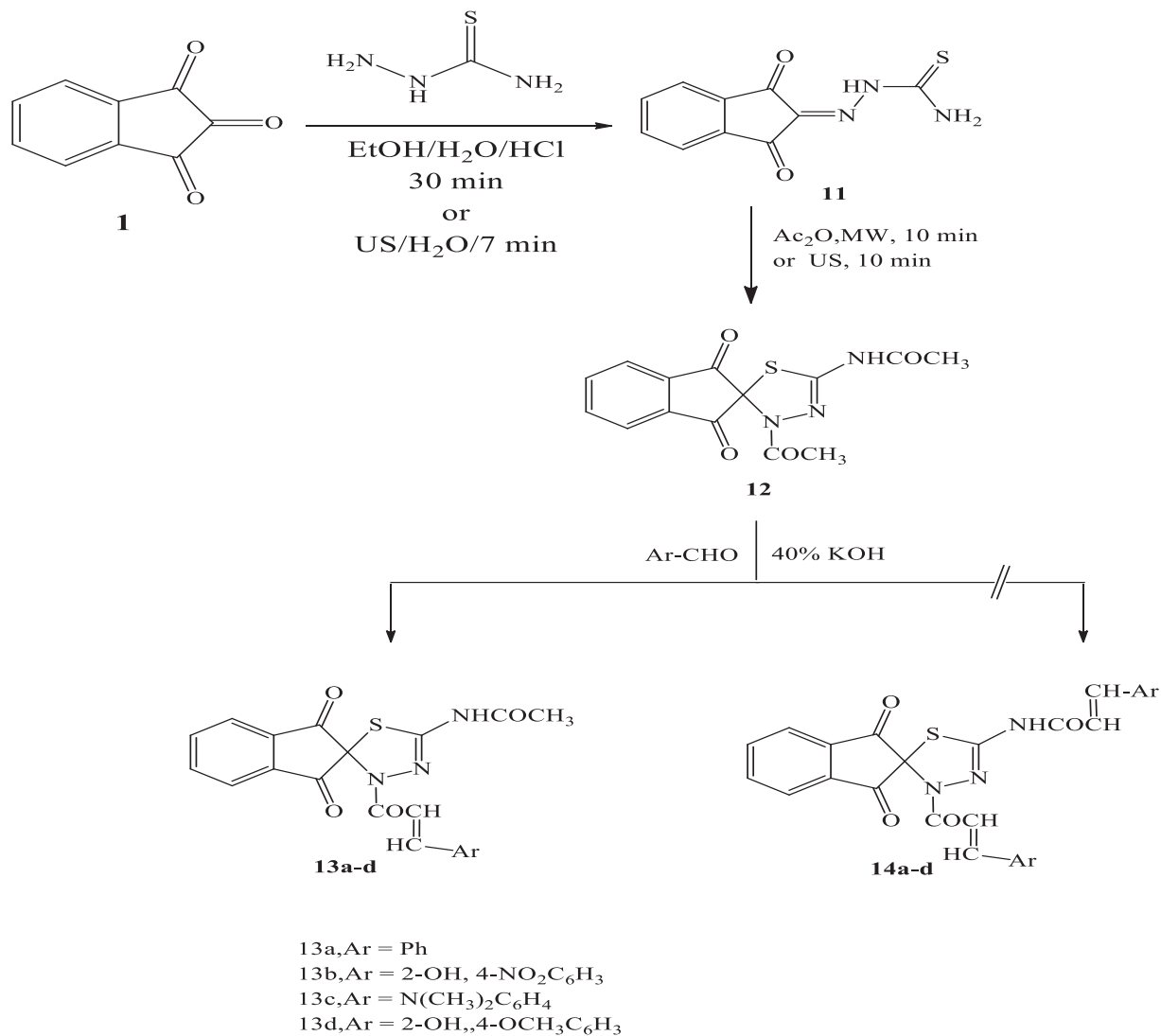
The synthesis of *N*-(3'-acetyl-1,3-dioxo-1,3-dihydro-3'*H*-spiro[indene-2,2'-[1,3,4]thiadiazol]-5'-yl)acetamide **12** from thiosemicarbazone derivative **11** has been obtained by mixing equimolar amounts of thiosemicarbazide and 1,2,3-indenetrione **1**, in ethanol/water in the existence of hydrochloric acid as a catalyst in a water bath for 30 min (Scheme 7) following the reported method (Reddy et al., 1985). This compound **11** could also be obtained by the sonication of ninhydrin and thiosemicarbazide in water at room temperature ($23\text{ }^\circ\text{C}$). This clean and efficient modified protocol allowed the formation of **11** in 99% within 7 min in pure form. Besides, by applying the ultrasonic irradiation tech-



Scheme 6 Synthesis of pyrazole derivatives **8–10**.

Table 1 Scaled-up synthesis of pyrazole derivative **8**.

Method	Yield (%)	YE (%)	CE (%)	RME (%)	AE (%)	PMI	E-Factor
Thermal	78	0.43	89.47	66.83	85.68	1.49	0.28
MW	98	9.80	89.47	83.96	85.68	1.19	0.02

**Scheme 7** Synthesis of compound (**12**) and chalcones **13a-d**.

nique as a sustainable energy source, the drawbacks of the reported methods such as harsh reaction conditions, longer reaction time, use of volatile carcinogenic organic solvents, and low yield were avoided. By using an excess amount of acetic anhydride (solvent and reactant), the obtained thiosemicarbazone derivative **11** underwent a cyclization reac-

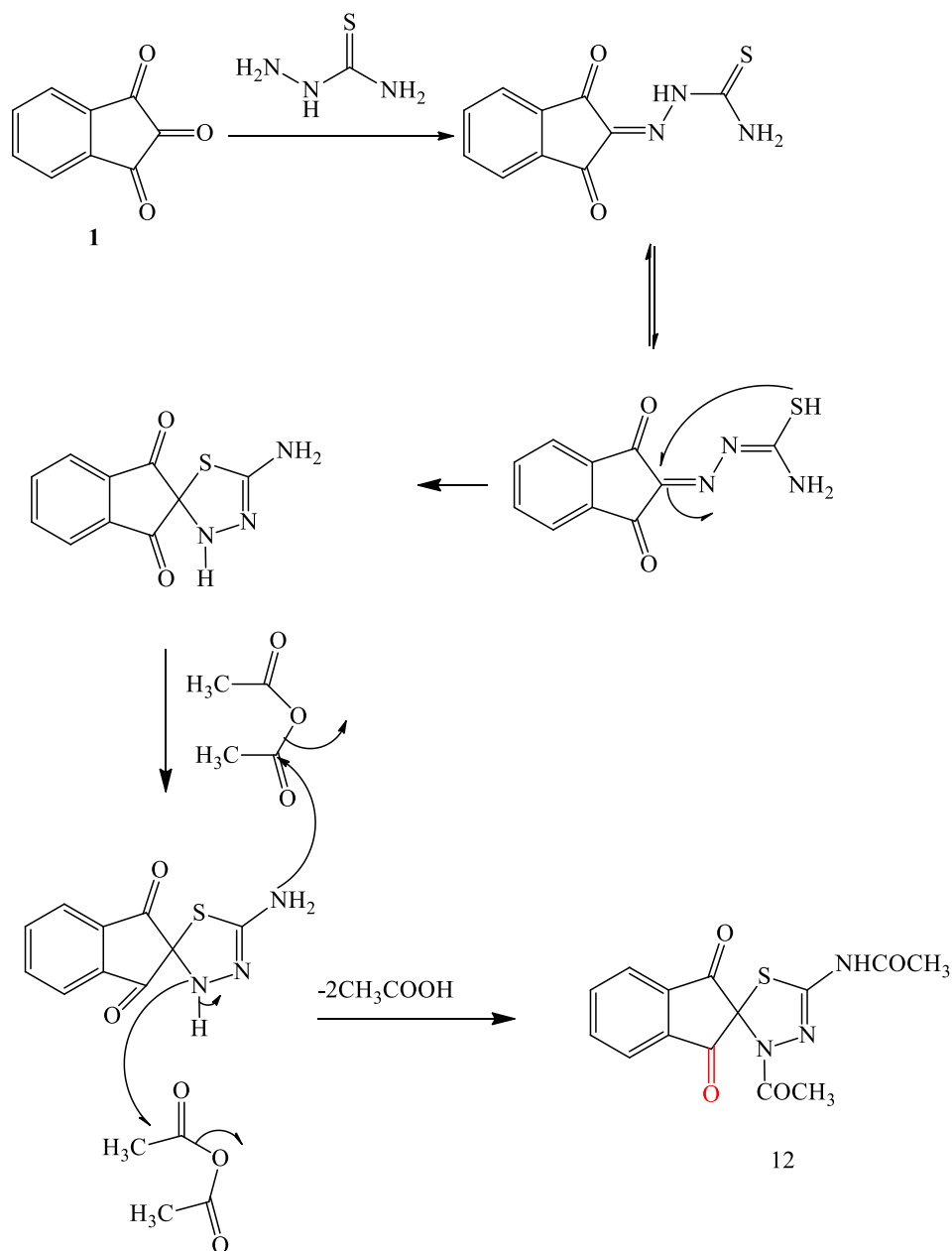
tion and subsequent acetylation under microwave irradiation into the unreported spiro[indene-2,2'-[1,3,4]thiadiazol]-5'-yl)acetamide derivative **12** in excellent yield (99%) and short reaction time (10 min), (**Scheme 7**). Interestingly, on performing the aforesaid reaction under ultrasonic irradiation condi-

tions, derivative **12** was obtained in 99% within 10 min at 50 °C (see Scheme 8).

The IR spectrum of derivative **12** displayed mainly a sharp strong absorption band around 1606 cm^{-1} which corresponds to the ninhydrin carbonyl groups with the disappearance of the amino (NH_2) and thiocarbonyl ($\text{C}=\text{S}$) bands and appearance of the medium absorption band at about 1716 cm^{-1} attributed to the stretching of the amide carbonyl groups. The ^1H NMR spectral analysis of the obtained compound **12**, two characteristic singlet signals at $\delta = 1.33$ and 2.0 ppm assigned to the two methyl groups. In addition, only one singlet at 10.58 ppm is attributed to the NH group, this is strong evidence to prove the cyclization of thiosemicarbazone, in view of the varied biological and pharmacological applications, we synthesized two unreported chalcone derivatives **13a-d** using Claisen Schmidt

condensation reaction. This reaction was carried out by the reaction of equimolar of the appropriate benzaldehyde with the acetyl derivative **12** in 40% NaOH solutions to produce the corresponding chalcones **13a-d** in excellent yields (Scheme 6) while the chalcone **14a-d** is not formed under the current reaction condition. The obtained products were characterized by using spectroscopic techniques such as IR and ^{13}C NMR spectra.

On the other hand, we synthesized series chalcone derivatives **13a, b** via reaction between benzaldehyde and the acetyl derivative **12** and were chosen as a template protocol (Scheme 7). Some variables for instance solvents, temperature, catalysts, and energy sources were investigated aiming to obtain the optimal reaction conditions. At first, the mixture of model reactants was refluxed in ethanol (20.0 mL) without



Scheme 8 A plausible Mechanism for formation of compound **12**.

adding a catalyst. Even after refluxing the reaction solution over a significant period, the generation of the predicted chalcone (**13a**) was not recognized under those same conditions (Table 2, entry 1). After charging the model reaction with a 40% NaOH solution as a promoter, a considerable yield (60%) of the intended product **13a** was achieved in 3 h (Table 2, entry 2). In repeating the same reaction but by using 40% KOH solution as catalyst instead of NaOH, the reaction rate slightly increased (Table 2, entry 3). The conversion of acetyl derivative **12** to the target chalcone **13a** was enhanced to 80% by sonicating the template reactants at room temperature (23 °C) for 15 min (Table 2, entry 4). The performance of the reaction was drastically reduced in solvents such as dioxane and DMF, generating the necessary product **13a** in lower yields however after 1 h of sonication (Table 2, entries 5 and 6). Water outperformed the other solvents evaluated for the present catalytic reaction (Table 2, entry 7). Diverse operational temperatures were utilized to enhance the efficiency of the current ultrasound-assisted protocol. The catalyst (KOH) successfully converted the modeled materials to the intended product **13a**, 94% in 10 min by elevating the temperature to 35 °C (Table 2, entry 8). It might be because the produced bubbles, which comprised catalyst and reactants, burst with significant energy to enhance both reaction yield and rate (Andraos, 2006). Surprisingly, increasing the temperature to 40 °C resulted in the required product **13a** being produced in perfect yield (99%) in just 8 min (Table 2, entry 9). Such finding is based on the fact that when the temperature of the reaction mixture increased, the viscosity and surface tension of the reaction mixture decreased, promoting the formation and collapse of bubbles (Protti et al., 2007). Surprisingly, at temperatures exceeding 50 °C, both reaction yield and rate are moderately reduced (Table 2, entries 10 and 11). At higher temperatures, additional bubbles were formed, which act as a barrier to the waves being successfully transferred across the reaction solution, affecting the conversion marginally (Protti et al., 2007). The time influence also was investigated, and the best duration was found to be 7 min.

To assess the feasibility of the current approach, the model reaction was carried out on a gram scale using the optimum conditions, yielding the required product **13a** in outstanding yield (98%, Scheme 7). Besides, diverse green measures such as Process Mass Intensity (PMI), Carbon Efficiency (CE), Reaction Mass Efficiency (RME), Atom Economy (AE), and E-factor (EF) were also studied (Scheme 7) to investigate the

present method in order of waste and carbon efficiency (Sheldon et al., 2007). The increased ecological suitability criteria, such as lower PMI (1.05) and EF (0.05) values, along with higher values of YE (14.14%), CE (100%), AE (95.74%), and RME (95.01%), verified the established protocol's eco-friendly strategy.

The optimal conditions were then employed for the assembly of series of chalcones using several aldehydes. Different benzaldehydes worked successfully in the reaction and produced high yields of the chalcones. Despite this, aromatic aldehydes with electron-donating groups **13c, d** yielded marginally less than those with electron-withdrawing groups **13b**. This observation may be owing to *o*-substituted benzaldehydes **13b; d** gave the required chalcone in slightly reduced yields, than the *p*-substituted derivative **13c**, probably due to steric factors. The chalcone derivatives were recrystallized from a proper solvent and characterized by using spectroscopic techniques such as FT-IR and NMR. The FT-IR spectrum of compound **13a** displayed bands at 1600, 1683, 2981, 3070 cm⁻¹ corresponding to (C=C), C=O, Ar-H and, NH, respectively. The ¹H NMR spectrum of derivative **13a** afforded signals at 1.29 and 10.23 ppm for CH₃, and NH, respectively. Treating the enones **13a,b** with phenylhydrazine which might be furnished either 4,5-dihydro-1*H*-pyrazoles **15a,b** or dehydrated products **16a,b**. Interestingly, the cyclocondensation reaction of chalcone derivatives **13a,b** with phenylhydrazine under refluxing conditions in ethanol afforded the unreported 4,5-dihydro-1*H*-pyrazoles **15a,b** as the major products (TLC) without the detection of dehydrated derivatives **16a,b** (Scheme 9). This observation might be explained based on the fact that the formation of 4,5-dihydro-1*H*-pyrazoles **15a, b**, were likely due to the electronic conjugation between the nitrogen atom (N1) lone pair of the pyrazoline-ring and the π -system of the phenyl motif that making the aromatization of the pyrazole ring quite complicated (Buriol et al., 2010). The structures of **15a, b** were confirmed by IR, ¹³C NMR analysis.

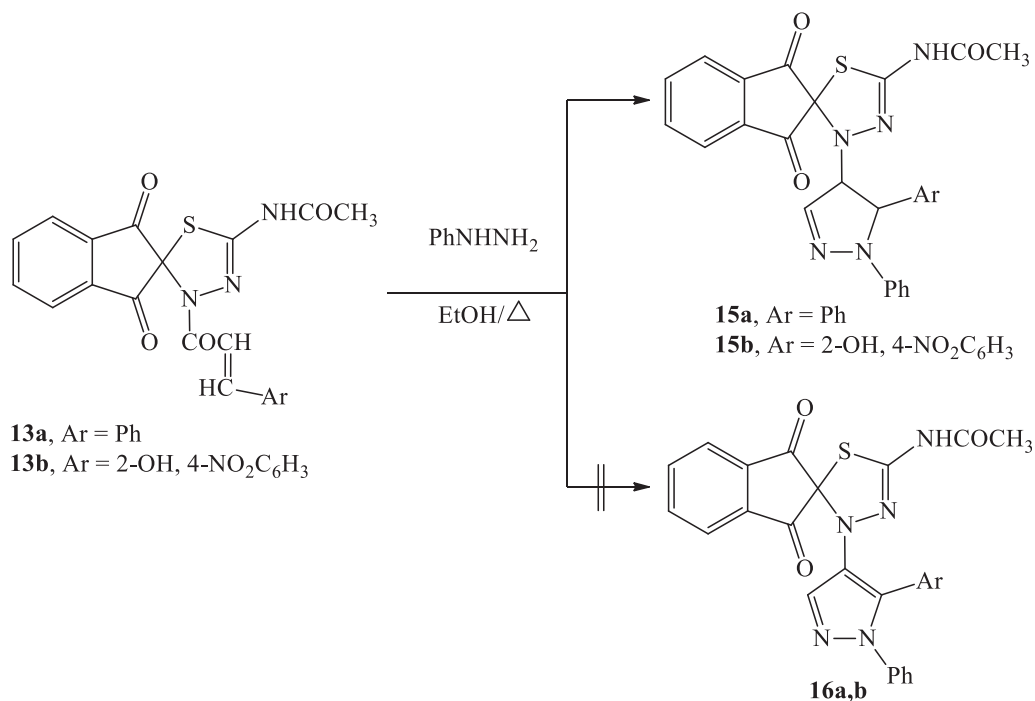
3.2. Antifungal potential

3.2.1. Antifungal activity and structure–activity relationship (SAR)

The newly synthesized compounds **1, 2a,b, 3, 4a,b, 5a-e, 7, 8, 9, 10, 12, 13a-d**, and **15a,b** were assayed *in-vitro* for their antifun-

Table 2 Reaction conditions optimization for the template reaction (Scheme 7).

Entry	Method	Catalyst	Solvent	Temp. (°C)	Time (min)	Yield (%)
	Silent	—	EtOH	100	180	0
	Silent	NaOH (40%)	EtOH	100	180	60
	Silent	KOH (40%)	EtOH	100	180	71
	US	KOH (40%)	EtOH	rt(23)	15	80
	US	KOH (40%)	Dioxane	rt(23)	60	65
	US	KOH (40%)	DMF	rt(23)	60	62
	US	KOH (40%)	H ₂ O	rt(23)	15	90
	US	KOH (40%)	H ₂ O	35	10	94
	US	KOH (40%)	H ₂ O	40	8	99
	US	KOH (40%)	H ₂ O	50	7	96
	US	KOH (40%)	H ₂ O	60	7	96
	US	KOH (40%)	H ₂ O	40	7	99



Scheme 9 Synthesis of pyrazole derivatives (**15a, b**).

gal activity towards *Fusarium oxysporum*, Metalaxyl was used as a reference to evaluate the potency of the tested compounds under the same conditions Fig. S3. The mean inhibition zone diameters (MIZ, mm/mg sample) ($n = 3$) were determined as a parameter of the antifungal activity, the antifungal results are illustrated in Fig.S3, recorded that all the novel compounds exhibited antifungal potential against *Fusarium oxysporum* fungi. The compounds **1** (MIZ = 80 mm), **7** (MIZ = 80 mm), and **4a** (MIZ = 75 mm) exhibited the highest antifungal effect and revealed a comparable potential to that shown by Metalaxyl. The structure-activity relationship (SAR) of the newly synthesized compounds **1**, **7**, and **4a** suggested that the withdrawing effect of the substituent groups in the synthesized compounds induced an increase in their antifungal activity compared to the others. For instance, the presence of carbonyl group as substituent attached directly to pyrimidine ring in compounds **1**, **7** and **4a** as electron-withdrawing groups showed a significant improvement against *Fusarium oxysporum* fungi. Compound **5a** (MIZ = 64 mm) showed moderate effect due to the presence of the nitro group replacement of the hydrogen atom present at the phenyl group. The results showed that the presence of electron-donating groups such as methyl, amino group, hydroxyl group at the pyrazole ring in compounds **8** (MIZ = 45 mm), **9** (MIZ = 50 mm) and **10** (MIZ = 38 mm) decreased their antifungal activities towards *Fusarium oxysporum* fungi.

3.2.2. Antifungal studies

On the other hand, we studied the efficacy of new synthetic chemical compounds against tomato damping-off disease caused by *Fusarium oxysporum*. The results indicated that the combination of six chemical compounds in the culture medium showed that the compound **1** has the strongest effect (86.5%), followed by **7**, **4a** and **5a-d** which have a percentage

of (81.2%), (78.8%) and (76.4%) respectively. In addition, results showed that **3** and **4b** of a lowest effect on the inhibition of *Fusarium oxysporum*. These chemical compounds showed an effective antifungal activity against *Fusarium oxysporum*. The chemical compound **12** showed lowest antifungal effect on *Fusarium oxysporum* (45%). While, chemical compound of **5a**, **5b**, **5c**, **13a**, and **13b**, have no any antifungal effect on *Fusarium oxysporum*. These results indicated that *F. oxysporum* was probably more sensitive to the chemical compounds **1**, **7**, **4a** and **5a** than chemical compound **12**. Moustafa and Elkanzi, 2021 evaluated the effect of Pyrazolo pyrimidine against *P. aphanidermatum*, which isolated from olive feeder roots. In addition study the ability of pyrazolo pyrimidine to decline the production of zoo-spores and oospores of the fungus. Their results observed that the synthetic chemical compound of pyrazolo pyrimidine inhibited mycelial growth and production of zoo- and oospores of *P. aphanidermatum*. The highest antifungal activity observed in pyrazolo pyrimidine is probably due to the presence of methyl group. So in this study the minimum inhibitory concentrations (MIC) was carried out to compare the effect of six chemical compound against *F. oxysporum*. Our in vitro tests showed that the treatments with **8**, **9**, **10**, **2a**, **2b**, **3**, **4b**, and **12** have no effects on the mycelial growth of *F. oxysporum* exposed to 10, 15, 25, and 50 mg/ml concentrations. Only chemical compounds of **1** and **7** were effective at low concentrations (10 mg/ml) 42 ± 0.24 and 42 ± 0.24 , respectively as compared to chemical compound **4a** and **5a** 38 ± 0.24 and 20 ± 0.1 , respectively. However, higher concentrations (100 mg/ml) of chemical compound **1** and **7** reduced mycelial growth of *F. oxysporum* (80 ± 0.14 , and 80 ± 0.14), respectively. In the comparison of the inhibitory effect of the various chemical compounds (**9**, **8**, **10**, **4b**, **4a**, **3**, **4b** and **12**) higher concentrations with 100 mg/ml reduced mycelial growth to 50 ± 0.14 , 45 ± 0.1 , 38 ± 0.3 ,

38 ± 0.2, 38 ± 0.12, 25 ± 0.2, 25 ± 0.2 and 42 ± 0.12, respectively (Table 3). The results of the present study demonstrated that MIC (25 µg/ml) of chemical compound 1 and 7 reduced mycelial growths in vitro; the percentage of reduction varied between 42 and 42% as compared to the control. Numerous formulated chemical compounds were shown to effectively reduce the pre damping off disease caused by of *F. oxysporum* and increase symptomless plant stand in controlled trials. The suppression of *F. oxysporum* development in the agar bottles corresponds with the ability of these chem-

ical compounds to reduce growth of *Fusarium* in agar bottles (Table 4 & fig. 8). The inhibitory effect of chemical compound 1 on fungal hyphal morphology was clearly detected by using Scanning electron microscopic. SEM images from the zone of interaction in culture showed the loss of structural integrity of the mycelium. A variety of aberrant features such as hyphal perforation, lysis, fragmentation and degradation of mycelia were observed in chemical compounds 1, 7, 4a and 5a. Higher concentrations (100 µg/ml) of chemical compound showing abnormal characters in *F. oxysporum* (fig 7).

Several studies have reported that chemical compound applications can suppress diseases caused by several pathogens (Boumaaza et al., 2015). The chemicals documented as generally regarded as safe (GRAS) by the United States Food and Drug Administration (FDA) are considered as non-toxic since wide historical use did not cause any health hazards. Salts such as sodium benzoate, sodium methylparaben, sodium bicarbonate and potassium sorbate are considered as GRAS and their antifungal activity can be applied as part of post-harvest. However, GRAS compounds are generally not considered as BCAs. In spite of they generally influence fungal cell membrane permeability and fungal nutrient transport but are non-toxic to humans and can be utilized as part of organic farming (Ons et al., 2020). The combined utilized of GRAS antagonists and fungicides, the addition of sodium bicarbonate to imazalil importantly improved its activity against both fungicide-sensitive and fungicide-resistant isolates of fungi on harvested lemons (Smilanick et al., 2005). Kanetis et al. (Moustafta and Elkanzi, 2021) mentioned that the efficiency of fungicides such as azoxystrobin, fludioxonil or pyrimethanil is significantly increased when mixed with GRAS sanitizers such as sodium bicarbonate when treating citrus green mold.

3.2.3. Isolation and molecular identification of damping-off fungi from infected tomato plants

F. oxysporum was one of the important pathogenic fungi present in soil observed adhering to tomato roots grown in the field studied. Identification of *F. oxysporum* was done based

Table 3 Effect of New tested synthetic compounds on the mycelium growth of *F. oxysporum* in solid (PDA) media at 28 °C after 7 days in the dark.

New synthetic chemical compound	Average of Diameter of inhibition zone / mm	Mycelial growth inhibition (%)
Metalaxyl (control)	85 ± 0.2	96.50
DMSO (control)	0	0
1	80 ± 0.21	94.1
4a	75 ± 0.1	88.2
7	80 ± 0.13	94.1
5a	64 ± 0.20	75.3
9	50 ± 0.56	58.8
8	45 ± 0.13	52.9
10	38 ± 0.21	44.7
4b	38 ± 0.10	44.7
2a	38 ± 0.13	44.7
3	25 ± 0.22	29.4
4b	25 ± 0.5	29.4
5b	0	0
5c	0	0
5d	0	0
5e	0	0
12	42 ± 0.14	49.4
13a	0	0
13b	0	0

Table 4 Mycelium growth of *F. oxysporum* exposed to different concentrations of chemical compounds (100, 50, 25, 15 and 10 µg/mL) for 7 days at 27 °C in dark.

Chemical compounds	Average of diameter of inhibition zone (100 µg/mL)	Average of diameter of inhibition zone (50 µg/mL)	Average of diameter of inhibition zone (25 µg/mL)	Average of diameter of inhibition zone (15 µg/mL)	Average of diameter of inhibition zone (10 µg/mL)
DMSO (control)	0	0	0	0	0
Metalaxyl (control)	85 ± 0.14	60 ± 0.20	45 ± 0.16	45 ± 0.1	45 ± 0.18
1	80 ± 0.14	57 ± 0.14	42 ± 0.09	42 ± 0.18	42 ± 0.24
4a	75 ± 0.14	50 ± 0.14	38 ± 0.09	38 ± 0.18	38 ± 0.24
7	80 ± 0.14	57 ± 0.14	42 ± 0.09	42 ± 0.18	42 ± 0.24
5a	64 ± 0.01	33 ± 0.4	20 ± 0.12	18 ± 0.16	20 ± 0.1
9	50 ± 0.14	20 ± 0.18	10 ± 0.20	5 ± 0.1	5 ± 0.16
8	45 ± 0.1	18 ± 0.12	10 ± 0.22	10 ± 0.14	5 ± 0.2
10	38 ± 0.3	10 ± 0.1	7 ± 0.12	7 ± 0.12	7 ± 0.12
2b	38 ± 0.2	12 ± 0.1	5 ± 0.24	5 ± 0.3	5 ± 0.2
2a	38 ± 0.12	12 ± 0.23	5 ± 0.18	5 ± 0.1	5 ± 0.12
3	25 ± 0.2	10 ± 0.12	5 ± 0.12	5 ± 0.11	5 ± 0.18
4b	25 ± 0.2	10 ± 0.2	5 ± 0.18	5 ± 0.1	5 ± 0.2
12	42 ± 0.12	17 ± 0.18	8 ± 0.2	8 ± 0.2	8 ± 0.18

on morphological criteria and molecular identification according to (Rahjoo et al., 2008) (Fig. 2). The sequence of the pathogenic fungi (N. JF 505) was closely related to *F. oxysporum* (Genbank accession number, MW830121) with 100% similarity (Fig. 3). (<https://www.ncbi.nlm.nih.gov/nuccore/MW830121.1?report=GenBank>).

3.2.4. The effect of tested chemical compounds on the mycelial growth of *Fusarium oxysporum*

Measuring of the inhibition zones around each tested synthetic chemical compound against *F. oxysporum* indicated that some of these chemical compounds showed inhibition zones around *F. oxysporum* growth on PDA medium at 27 °C in the dark.

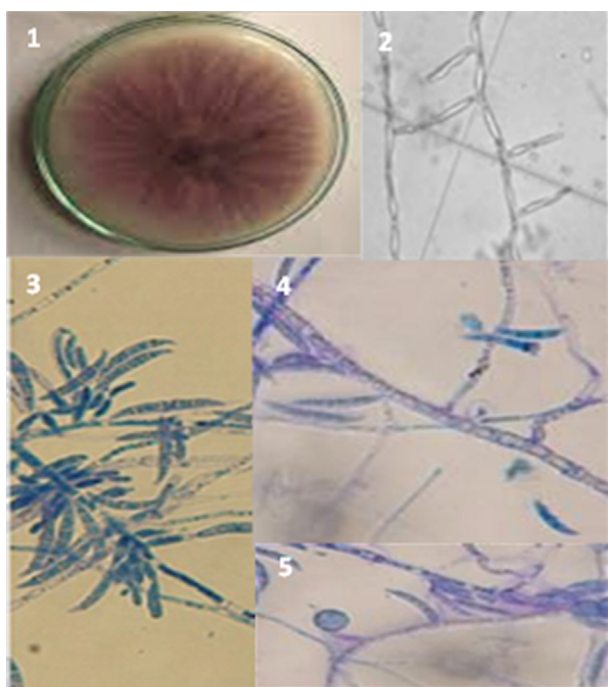


Fig. 2 Cultural and morphological structures of *Fusarium oxysporum*. (1) Colony aspect on PDA medium. (2) Monophialides. (3) Macroconidia. (4) Macroconidia. (5) Chlamydospores.

The compounds **1** and **7** displayed the strongest effect (80.5%), followed by, **4a** and **5a** were (75%) and (64 %) respectively. In addition, results showed that **3** and **4b** having the lowest effect on the inhibition of pathogenic isolated fungus. Other chemical compounds showed inhibition zones between 40 and 25 mm (Table 3, Fig. S1).

The minimum inhibitory concentrations (MIC) were determined and are given in Table 4; figure (S2, S3). The most active compound was **1**, which presents against *F. oxysporum*, has value 25 µg/mL.

3.2.4.1. Micrograph of *Fusarium oxysporum* grown in tested chemical compound concentrations. The scanning electron microscopy analysis revealed that tested chemical compound (**1**) 25 µg/mL induced marked effects on the morphology and density of mycelium of *F. oxysporum*. Fig. S4 shows a greater morphological change as deformation of the mycelium perforation, lysis of cell and destruction of both mycelium and conidia of *F. oxysporum*; when compared to the control. While the Effect of adding tested chemical compounds on pre-emergence damping-off by *F. oxysporum*- In agar bottles indicate that Controlling damping-off of tomato seeds caused by *F. oxysporum*, by different new chemical compounds add to 2% water agar medium were showed in (Tables 5, fig S5, S6). All tested chemical compounds reduced the pre damping off disease caused by *F. oxysporum*, but in different ranges. The effective tested chemical compounds were **1** which improved seeds emergence when subjected to the tested pathogenic fungi and reduced the disease to 94%; chemical compounds **4a** and **5a** reduced the disease to 88%. The least chemical compounds were **3** and **4b** which reduced the disease to only 61%.

3.3. Docking study

Succinate dehydrogenase (EC 1.3.5.1) is involved in Krebs cycle and respiration chain via catalysing the oxidation of succinate to fumarate in the mitochondrial matrix (Pollard et al., 2003; Yu et al., 2020). SDH is considered as a promising target for agrochemical discovery due to its essential role in life processes (Guan et al., 2014; Jeschke, 2018).

Molecular docking analysis was performed within succinate dehydrogenase (SDH) as a target enzyme in order to

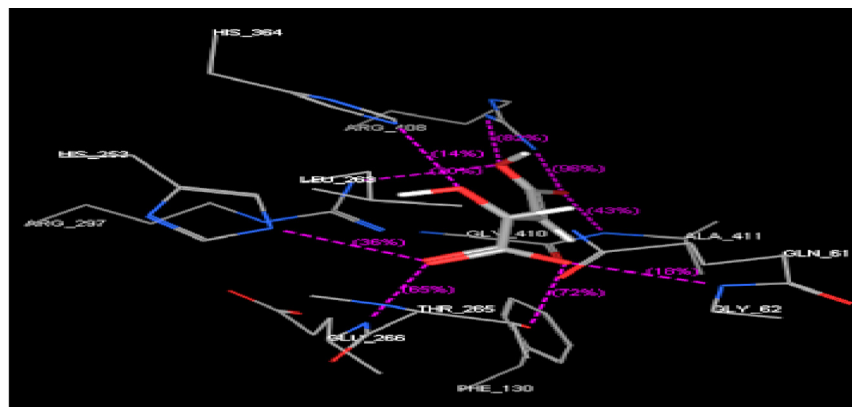
```
g c g g a g g g a t   c a t t a c c g a g   t t a c a a c t c   c a a a c c c c t   g t g a a c a t a c   c a c t t g t t g c   c t c g g c g g a t   c a g c c c g c t c
c c g g t a a a a c   g g g a c g g c c c   g c c a g a g g a c   c c t a a a c t c   t g t t t c t a t a   t g t a a c t t c t   g a g t a a a a c c   a t a a t a a a t
c a a a a c t t t c   a a c a a c g g a t   c t c t t g g t t c   t g g c a t c g a t   g a a g a a c g c a   g c a a a t g c g   a t a a g t a a t g   t g a a t t g c a g
a a t t c a g t g a   a t c a t c g a a t   c t t t g a a c g c   a c a t t g c g c c   c g c c a g t a t t   c t g g c g g g c a   t g c c t g t t c g   a g c g t c a t t t
c a a c c c t c a a   g c a c a g c t t g   g t g t t g g g a c   t e g c g t t a a t   t e g c g t t c e t   c a a a t t g a t t   g g c g g t c a c g   t c g a g c t t c c
a t a g c g t a g t   a g t a a a a c c c   t e g t t a c t g g   t a a t c g t e g c   g g c c a c g c c g   t t a a a c c c a   a c t t e t g a a t   g t t g a c c t c g
g a t c a g g t a g   g a a t a c c c g c   t g a a c t t a a g   c a t a t c
```

Fig. 3 Sequence analysis of the ITS1-5.8S rRNA-ITS2 region of *F. oxysporum*.

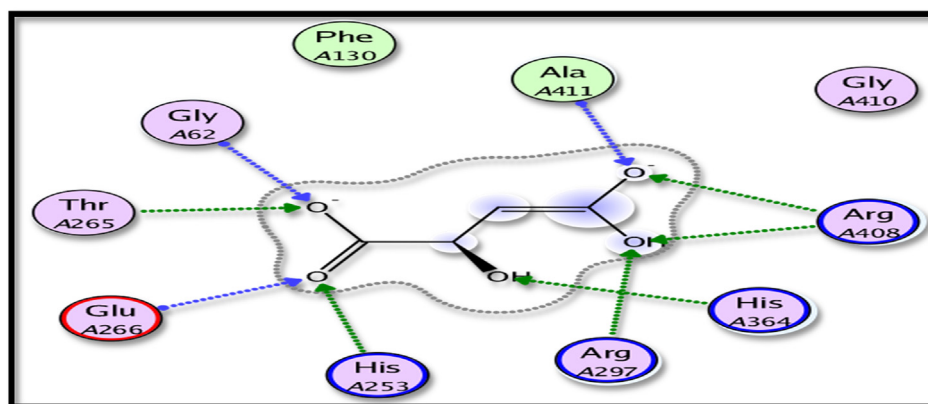
Table 5 Effect of tested chemical compounds (25 µg/mL) on pre-emergence damping-off disease of Tomato seeds grown on 2% water agar medium.

Treatment	Percentage of germination (PG)	Percent disease incidence (PDI)
Control : seeds without pathogenic fungi	100%	0%
Control : seeds with pathogenic fungi only	13%	86%
Seeds with Pathogenic fungi + 1	94%	7%
Seeds with Pathogenic fungi + 4a	88%	13%
Seeds with Pathogenic fungi + 7	83%	17%
Seeds with Pathogenic fungi + 5a	88%	12%
Seeds with Pathogenic fungi + 9	77.8%	25%
Seeds with Pathogenic fungi + 8	77.8%	24%
Seeds with Pathogenic fungi + 10	66%	35%
Seeds with Pathogenic fungi + 2b	66%	35%
Seeds with Pathogenic fungi + 2a	66%	35%
Seeds with Pathogenic fungi + 3	61%	42%
Seeds with Pathogenic fungi + 4b	61%	45%
Seeds with Pathogenic fungi + 12	72.2%	28%

*Standard error for 3 replicates.



(A)



(B)

Fig. 4 The suggested binding of the cocrystallized ligand within SDH active site. A) 3D, B) 2D binding interaction.

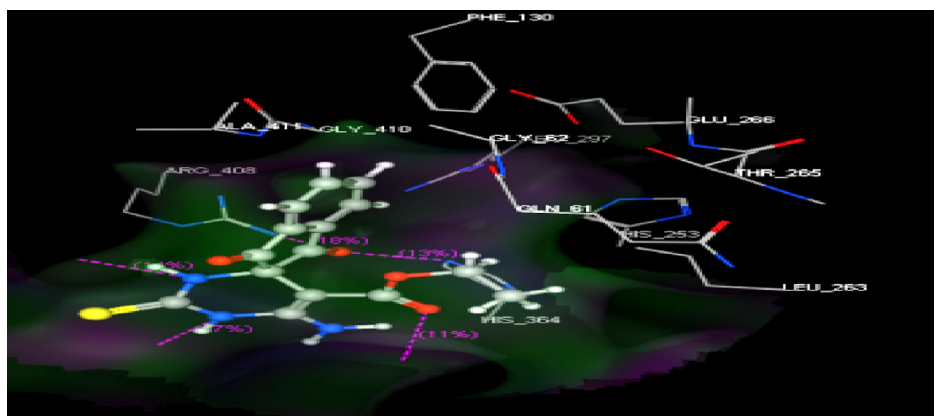
rationalize the promising findings obtained for the active compounds **1**, **2a,b**, **5a**, **5b-d**, **7**, **8**, **9**, **10**, **12**, **13a** using MOE, 2008, Chemical Computing Group Inc. The crystal structure of SDH with the cocrystallized ligand was downloaded from Protein Data Bank (code: 2FBW). The cocrystallized ligand (malate like intermediate) was redocked within SDH with root mean standard deviation (RMSD) = 1.5707. The main binding interactions resulted in hydrogen bondings with Ala411, Arg408, His364, Arg297, His253, Glu266, Thr265 and Gly62 (Fig. 4).

The formed hydrogen bonds and binding energy scores obtained from docking study are recorded in Table 6. From the docking results, compound (**1**) displayed the highest binding energy (-16.34 kcal/mol) with His56, Glu397, Ser413, Arg408 and His364 through binding with ester C=O, 2NH of pyrimidine ring and indene C=O (Fig. 5).

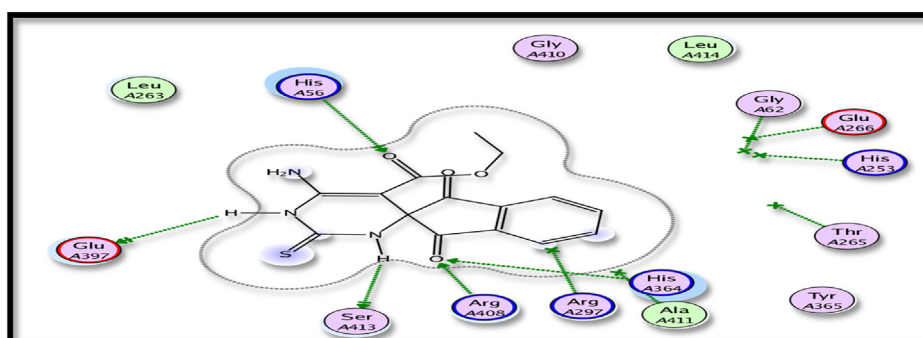
Furthermore, compound (**7**) exhibited good fitting with SDH binding site with binding energy score = -14.99 kcal/mol. In addition, this candidate (**7**) revealed six H-bonds as followings (Fig. S7):

Table 6 Docking study results for the newly synthesized compounds.

Compound	Affinity Kcal/mol	No. of hydrogen bonds	Distance (Å) from the main residue	Functional group	
1	-16.34	5	His56	2.97	Ester C=O
			Glu397	2.27	NH
			Ser413	3.07	NH
			Arg408	2.99	Indene C=O
			His364	3.01	Indene C=O
7	-15.99	6	His364	2.98	Hydrazide C=O
			Gln61	2.75	Indene C=O
			Arg297	2.56	Hydrazide C=O
			Arg408	3.05	Hydrazide C=O
			Ala411	3.11	NH ₂
			Arg408	3.22	NH ₂
2b	-12.65	3	Arg408	2.98	Pyrimidine C=O
			Arg297	2.51	Pyrimidine C=O
2a	-12.34	3	His364	3.17	Pyrimidine C=O
			Ser413	2.98	Pyrimidine C=O
			His364	3.11	Pyrimidine C=O
8	-14.19	5	Arg408	2.92	Pyrimidine C=O
			His56	3.24	OH
			Thr224	3.05	OH
			His56	2.98	NH ₂
			Arg408	2.72	C=O
9	-15.09	5	His364	3.11	C=O
			His56	2.59	Pyrimidine NH ₂
			Thr224	2.84	Pyrazole NH ₂
			Ala59	2.98	OH
			His364	3.04	Indene C=O
			Arg408	3.15	Indene C=O
10	-11.87	4	Arg408	2.35	Amide C=O
			Arg408	2.94	Indene C=O
			Ser413	2.80	NH ₂
			His364	2.77	Indene C=O
5a	-15.78	3	Arg408	2.98	C=O
			Arg297	2.78	C=O
			His364	3.09	C=O
5b	-12.59	2	Gly62	3.09	OCH ₃
			Thr265	2.93	OCH ₃
3	-11.45	3	Gln61	3.22	Oxazine C=O
			His364	2.98	Indene C=O
			Arg408	2.83	Indene C=O
12	-14.84	4	His364	2.85	Indene C=O
			Arg408	2.74	Acetyl C=O
			Ala411	2.94	Acetyl C=O
			Ser413	3.06	Amide C=O
Cocrystallized Ligand	-15.40	9	Gly62	2.58	OH
			Thr265	2.56	OH
			Glu266	2.99	C=O
			His253	2.93	C=O
			Arg297	3.06	OH
			His364	3.18	OH
			Arg408	2.98	OH
			Arg408	2.63	C=O
			Ala411	2.63	OH



(A)



(B)

Fig. 5 The suggested binding of compound **1** within SDH active site. A) 3D, B) 2D binding interaction.

- i) His364 with hydrazide C=O
- ii) Gln61 with indene C=O
- iii) Arg297 with hydrazide C=O
- iv) Arg408 with hydrazide C=O
- v) Ala411 with NH₂
- vi) Arg408 with NH₂

Compound **5a** recorded three H bonds with Arg408, Arg297 and His364 through binding with indene C=O moiety, in addition to the formation of arene cation interaction between Arg297 and the phenyl moiety (Fig. S8). The target compound **2b** formed three H-bonds with Arg297, Arg408 and His364 through interaction with pyrimidine C=O. This candidate **2b** displayed also two arene cation interactions with Arg408 and His364 with binding energy score = -12.65 Kcal/mol (Fig. S9). Furthermore, compound **2a** displayed arene cation interaction with phenyl ring. Also, it showed three H-bonds as follows: i) His364 with C=O, ii) Arg408 with C=O and iii) Ser413 with C=O (Fig. S10). In addition, the target compound **8** showed five H-bonds with His56, Thr224, Arg408 and His364 amino acids with binding energy score equals to -15.29 Kcal/mol (Fig. S11). Moreover, derivative **9** showed good fitting inside SDH enzyme displaying five hydrogen bonds as follows: i) His56 with pyrimidine NH₂, ii) Ala59 with OH, iii) Thr224 with pyrazole NH₂, iv) His364 with indene C=O, and vi) Arg408 with indene C=O. in addition,

the benzene ring of indene formed arene cation interaction with Arg408 (Fig. S12). The candidate **10** recorded binding energy score = -11.39 kcal/mol and the pyrazole moiety formed hydrophobic interaction with His364. Also, this candidate **10** demonstrated four H-bonds with Arg408, Ser413, and His364 through binding with carbonyl moieties and amino group (Fig.S13). On the other hand, the candidate **5b** revealed only two H-bonds with Gly62 and Thr265 via binding with methoxy group and exhibited also arene cation interaction with the phenyl moiety (Fig. S14). On the other hand, the target compound **3** displayed three H-bond with Arg408, His364 and Gln61 through carbonyl moieties with binding energy = 11.45 kcal/mol (Fig. S15). Finally, the thiadiazole candidate **12** displayed good fitting inside SDH active site with binding energy score = -14.84 kcal/mol. Furthermore this compound showed four H-bonds with His364, Ala411, Arg408, and Ser413 in addition to formation arene cation interaction between Arg297 and the benzene moiety (Fig. S16).

In conclusion, all the docked target compounds displayed good binding within succinate dehydrogenase enzyme with docking scores = -16.34- -11.45 kcal/mol comparing with the cocrystallized ligand which recorded binding energy score = -15.40 kcal/mol). Furthermore, all the compounds showed 2 to 6 hydrogen bonds within the binding site. Moreover, compounds **1** and **7** (the most active candidates) revealed the best docking scores (-16.34 and -15.99 kcal/mol, respec-

tively) and recorded 5 and / or 6 hydrogen bonds within the active site. In addition, compound **3** (the least active candidate) demonstrated the least docking score = -11.45 kcal/mol and formed 3 hydrogen bonds. These outcomes were in agreement with that recorded by antifungal studies.

4. Conclusion

Sustainable and simple preparation of spiro [indene-2,4'-pyrimidine]-5'-carboxylate **1** was achieved by microwave irradiation of ninhydrin, thiourea, and ethyl cyanoacetate. The target compound **1** had been characterized by FT-IR and NMR, and Mass spectra. An excellent reaction yield (96%) was obtained in the presence of potassium carbonate and irradiation with microwave for 20 min. Also, pyrazole derivatives (**8**, **9**, and **10**) were prepared in excellent yields (98, 96, and 99%, respectively) *via* microwave irradiation of derivative **7** with ethyl acetoacetate, ethyl cyanoacetate, and diethyl malonate. The green synthesis of the spiroacetamide derivative (**12**) *via* acetylation of thiosemicarbazone derivative **11** under microwave irradiation provided **12** in an excellent yield (99%). Besides, chalcone **13a-d** was prepared in excellent yield *via* ultrasonic irradiation of **12** with aromatic aldehydes. The reaction of compounds **13a-b** with phenylhydrazine provided **15a-b**. The molecular docking study of the synthesized compound indicated the active compounds are **1**, **2a**, **2b**, **5a**, **5b-d**, **7**, **8**, **9**, **10**, **12**, and **13a**. Ethyl 6'-amino-1,3-dioxo-2'-thioxo-1,2',3,3',5',6'-hexahydro-1'*H*-spiro[indene-2,4'-pyrimidine]-5'-carboxylate **1** is considered as new effective regulators of vegetative growth of tomato depending on their evaluation against tomato damping-off disease caused by *Fusarium oxysporum*.

Declaration of Competing Interest

The authors declare that they have no known competing financial interests or personal relationships that could have appeared to influence the work reported in this paper.

Acknowledgements

The financial support from Deanship of graduate studies at Jouf University for funding and supporting this research, through the initiative of DGS, Graduate students research support (GSR) at Jouf university, Saudi Arabia.

Appendix A. Supplementary data

Supplementary data to this article can be found online at <https://doi.org/10.1016/j.arabjc.2022.103731>.

References

- Muhammad, A.Z., Masaret, G.S., Amin, M.M., Abdallah, M.A., Farghaly, T.A., 2017. Anti-inflammatory, analgesic and anti-ulcerogenic activities of novel bis-thiadiazoles, bis-thiazoles and bis-formazanes. *Med. Chem.* 13, 226–238.
- Abdelgawad, M.A., Bakr, R.B., Ahmad, W., Al-Sanea, M.M., Elshemy, H.A., 2019. New pyrimidine-benzoxazole/benzimidazole hybrids: Synthesis, antioxidant, cytotoxic activity, in vitro cyclooxygenase and phospholipase A2-V inhibition. *Bioorg. Chem.* 92, 103218.
- Abdelgawad, M.A., Bakr, R.B., Azouz, A.A., 2018. Novel pyrimidine-pyridine hybrids: synthesis, cyclooxygenase inhibition, anti-inflammatory activity and ulcerogenic liability. *Bioorg. Chem.* 77, 339–348.
- Abdellatif, K.R., Bakr, R.B., 2020. Pyrimidine and fused pyrimidine derivatives as promising protein kinase inhibitors for cancer treatment. *Med. Chem. Res.*, 1–19.
- Abo-Elyousr, K.A., Mohamed, H.M., 2009. Note biological control of Fusarium wilt in tomato by plant growth-promoting yeasts and rhizobacteria. *Plant Pathol. J.* 25, 199–204.
- Al-ani, R.A., Adhab, M.A., Hamad, S.A., Diwan, S.N., 2011. Tomato yellow leaf curl virus (TYLCV), identification, virus vector relationship, strains characterization and a suggestion for its control with plant extracts in Iraq. *Afr. J. Agric. Res.* 6, 5149–5155.
- Al-Sanea, M., Parambi, D., Shaker, M., Elsherif, H., Elshemy, H., Bakr, R., Al-Warhi, T., Gamal, M., Abdelgawad, M., 2020. Design, Synthesis, and In Vitro Cytotoxic Activity of Certain 2-[3-Phenyl-4-(pyrimidin-4-yl)-1-H-pyrazol-1-yl] acetamide Derivatives. *Russ. J. Org. Chem.* 56, 514–520.
- Andraos, J., 2006. On using tree analysis to quantify the material, input energy, and cost throughput efficiencies of simple and complex synthesis plans and networks: Towards a blueprint for quantitative total synthesis and green chemistry. *Org. Process Res. Dev.* 10, 212–240.
- B Bakr, R., BM Mehany, A., RA Abdellatif, K., 2017. Synthesis, EGFR Inhibition and Anti-cancer Activity of New 3, 6-dimethyl-1-phenyl-4-(substituted-methoxy) pyrazolo [3, 4-d] pyrimidine Derivatives. *Anti-Cancer Agents in Medicinal Chemistry (Formerly Current Medicinal Chemistry-Anti-Cancer Agents)* 17, 1389–1400.
- Bakr, R.B., Azab, I.H.E., Elkanzi, N.A.A., 2021. Thiochromene candidates: design, synthesis, antimicrobial potential and in silico docking study. *J. Iranian Chem. Soc.*, 1–11.
- Bakr, R.B., Elkanzi, N.A., 2020. Preparation of some novel thiazolidinones, imidazolinones, and azetidinone bearing pyridine and pyrimidine moieties with antimicrobial activity. *J. Heterocycl. Chem.* 57, 2977–2989.
- Bakr, R.B., Elkanzi, N.A.A., Ghoneim, A.A., Moustafa, S., 2018. Synthesis, MOLECULAR DOCKING STUDIES AND IN VITRO ANTIMICROBIAL EVALUATION OF NOVEL PYRIMIDO [1, 2-A] QUINOXALINE AND TRIAZINO [4, 3-a] Quinoxaline derivatives. *Heterocycles: Int. J. Rev. Commun. Heterocyclic Chem.* 96, 1941–1957.
- Bano, B., Khan, K.M., Begum, F., Lodhi, M.A., Salar, U., Khalil, R., Ul-Haq, Z., Perveen, S., 2018. Benzylidene indane-1, 3-diones: As novel urease inhibitors; synthesis, in vitro, and in silico studies. *Bioorg. Chem.* 81, 658–671.
- Boumaaza, B., Benkhelifa, M., Belkhouja, M., 2015. Effects of two salts compounds on mycelial growth, sporulation, and spore germination of six isolates of *Botrytis cinerea* in the western north of Algeria. *Int. J. Microbiol.*, 2015.
- Buriol, L., Frizzo, C.P., Marzari, M.R., Moreira, D.N., Prola, L.D., Zanatta, N., Bonacorso, H.G., Martins, M.A., 2010. Pyrazole synthesis under microwave irradiation and solvent-free conditions. *J. Braz. Chem. Soc.* 21, 1037–1044.
- Campos, M.D., Félix, M.d.R., Patanita, M., Materatski, P., Varanda, C., 2021. High throughput sequencing unravels tomato-pathogen interactions towards a sustainable plant breeding. *Horticult. Res.*, 8.
- Catto, M., Aliano, R., Carotti, A., Cellamare, S., Palluotto, F., Purgatorio, R., De Stradis, A., Campagna, F., 2010. Design, synthesis and biological evaluation of indane-2-arylhydrazinyl-methylene-1, 3-diones and indol-2-aryldiazinylmethylene-3-ones as β -amyloid aggregation inhibitors. *Eur. J. Med. Chem.* 45, 1359–1366.
- de Oliveira, A.S., Gazolla, P.A., Oliveira, A.F.C.d.S., Pereira, W.L., de S. Viol, L.C., Maia, A.F.d.S., Santos, E.G., da Silva, Í.E., Mendes, T.A.d.O., da Silva, A.M., 2019. Discovery of novel West Nile Virus

- protease inhibitor based on isobenzonafuranone and triazolico derivatives of eugenol and indan-1, 3-dione scaffolds. *PLoS one* 14:e0223017.
- El-Naggar, M., Sallam, H.A., Shaban, S.S., Abdel-Wahab, S.S., E Amr, A.E.-G., Azab, M.E., Nossier, E.S., Al-Omar, M.A., 2019. Design, synthesis, and molecular docking study of novel heterocycles incorporating 1, 3, 4-thiadiazole moiety as potential antimicrobial and anticancer agents. *Molecules* 24, 1066.
- Elkanzi, N.A.A., Bakr, R.B., 2020. Microwave Assisted, Antimicrobial Activity and Molecular Modeling of Some Synthesized Newly Pyrimidine Derivatives Using 1, 4-diazabicyclo [2.2. 2] octane as a Catalyst. *Lett. Drug Des. Discovery* 17, 1538–1551.
- Elkanzi, N.A., Bakr, R.B., Ghoneim, A.A., 2019a. Design, Synthesis, Molecular Modeling Study, and Antimicrobial Activity of Some Novel Pyrano [2, 3-b] pyridine and Pyrrolo [2, 3-b] pyrano [2.3-d] pyridine Derivatives. *J. Heterocycl. Chem.* 56, 406–416.
- Elkanzi, N.A.A., Hrichi, H., Bakr, R.B., Hendawy, O., Alruwaili, M. M., Alruwaili, E.D., Almamtrfi, R.W., Alsharary, H.K., 2020. Synthesis, in vitro evaluation and molecular docking of new pyrazole derivatives bearing 1, 5, 10, 10a-tetrahydrobenzo [g] quinoline-3-carbonitrile moiety as potent antibacterial agents. *J. Iranian Chem. Soc.*, 1–15.
- Elkanzi, N.A.A., Ghoneim, A.A., Bakr, R.B., 2019b. Design, efficient synthesis and antimicrobial evaluation of some novel Pyrano [2, 3-b][1, 8] Naphthyridine and Pyrrolo [2, 3-f][1, 8] naphth-yridine derivatives. *Pharma Chem.* 11, 6–13.
- Fadda, A.A., Abd El Salam, M., Tawfik, E.H., Anwar, E., Etman, H., 2017. Synthesis and insecticidal assessment of some innovative heterocycles incorporating a thiadiazole moiety against the cotton leafworm, *Spodoptera littoralis*. *RSC Adv.* 7, 39773–39785.
- Ghoneim, A.A., Elkanzi, N.A., Bakr, R.B., 2018. Synthesis and studies molecular docking of some new thioxobenzo [g] pteridine derivatives and 1, 4-dihydroquinoxaline derivatives with glycosidic moiety. *J. Taibah Univ. Sci.* 12, 774–782.
- Ghoneim, A.A., El-Faragy, A.F., Bakr, R.B., 2020. Design, Synthesis, Molecular Docking of Novel Substituted Pyrimidinone Derivatives as Anticancer Agents. *Polycyclic Aromatic Compd.*, 1–17
- Giles, D., Karki, R., Sheeba, F., Venkatesh, D., Gurubasavarajawamy, P., 2011. Heterocyclic Indane-1, 3-Dione Derivatives as Topical Anti-Inflammatory Agents. *J. Pharmaceut. Sci. Res.* 3, 1253.
- Guan, A., Liu, C., Yang, X., Dekeyser, M., 2014. Application of the intermediate derivatization approach in agrochemical discovery. *Chem. Rev.* 114, 7079–7107.
- Hrichi, H., Ahmed, E.N.A., Badawy, B.R., 2020. Novel β -lactams and thiazolidinone derivatives from 1, 4-dihydroquinoxaline schiff's base: synthesis, antimicrobial activity and molecular docking studies. *Chem. J. Moldova* 15, 86–94.
- Hmouni, A., Hajlaoui, M.R., Mlaiki, A., 1996. Résistance de *Botrytis cinerea* aux benzimidazoles et aux dicarboximides dans les cultures abritées de tomate en Tunisie. *EPPO Bull.* 26 (3–4), 697–705.
- Jeschke, P., 2018. Current status of chirality in agrochemicals. *Pest Manag. Sci.* 74, 2389–2404.
- Kaiwart, S., Toppo, S., Sahu, S., 2020. Evaluation of tomato (*Solanum lycopersicum* L.) Hybrids for quality parameter in Allahabad agroclimatic condition. *J. Pharmacogn. Phytochem.* 9, 2089–2091.
- Karthika, S., Varghese, S., Jisha, M., 2020. Exploring the efficacy of antagonistic rhizobacteria as native biocontrol agents against tomato plant diseases. *3 Biotech* 10, 1–17.
- Keerthi Kumar, C.T., Keshavayya, J., Rajesh, T.N., Peethambar, S. K., Shoukat Ali, A.R., 2013. Synthesis, characterization, and biological activity of 5-phenyl-1, 3, 4-thiadiazole-2-amine incorporated azo dye derivatives. *Organ. Chem. Int.*, 2013.
- Kouzi, O., Pontiki, E., Hadjipavlou-Litina, D., 2019. 2-Arylidene-1-indandiones as Pleiotropic Agents with Antioxidant and Inhibitory Enzymes Activities. *Molecules* 24, 4411.
- Kumar, S., Nehra, M., Dilbaghi, N., Marrazza, G., Hassan, A.A., Kim, K.-H., 2019. Nano-based smart pesticide formulations: Emerging opportunities for agriculture. *J. Control. Release* 294, 131–153.
- Kundu, A., Pramanik, A., 2014. Synthesis of different isoindolone embedded heterocycles with phenolic subunits from a common intermediate, 3-(2'-hydroxyaroyl)-2, 3-dihydroisoindol-1-ones. *Tetrahedron Lett.* 55, 4466–4474.
- Lamichhane, J.R., Dürr, C., Schwanck, A.A., Robin, M.-H., Sarthou, J.-P., Cellier, V., Messéan, A., Aubertot, J.-N., 2017. Integrated management of damping-off diseases. A review. *Agron. Sustain. Develop.* 37, 10.
- Liu, T.T., Lee, R.E., Barker, K.S., Lee, R.E., Wei, L., Homayouni, R., Rogers, P.D., 2005. Genome-wide expression profiling of the response to azole, polyene, echinocandin, and pyrimidine antifungal agents in *Candida albicans*. *Antimicrob. Agents Chemother.* 49, 2226–2236.
- Maddila, S., Gorle, S., Seshadri, N., Lavanya, P., Jonnalagadda, S.B., 2016. Synthesis, antibacterial and antifungal activity of novel benzothiazole pyrimidine derivatives. *Arabian J. Chem.* 9, 681–687.
- Mandal, N., Sinha, A., 1992. An alternative approach for the chemical control of Fusarium wilt of tomato. *Indian Phytopathol.* 45, 194–198.
- Maurya, S., Dubey, S., Kumari, R., Verma, R., 2019. Management tactics for fusarium wilt of tomato caused by *Fusarium oxysporum* f. sp. *lycopersici* (Sacc.): A review. *Management* 4, 1–7.
- McGovern, R., 2015. Management of tomato diseases caused by *Fusarium oxysporum*. *Crop Prot.* 73, 78–92.
- McGovern, R., Vavrina, C., Noling, J., Datnoff, L., Yonce, H., 1998. Evaluation of application methods of metam sodium for management of Fusarium crown and root rot in tomato in southwest Florida. *Plant Dis.* 82, 919–923.
- Meena, K., Kumari, S., Khurana, J.M., Malik, A., Sharma, C., Panwar, H., 2017. One pot three component synthesis of spiro [indolo-3, 10'-indeno [1, 2-b] quinolin]-2, 4, 11'-triones as a new class of antifungal and antimicrobial agents. *Chin. Chem. Lett.* 28, 136–142.
- Millan, M.J., Gobert, A., Roux, S., Porsolt, R., Meneses, A., Carli, M., Di Cara, B., Jaffard, R., Rivet, J.-M., Lestage, P., 2004. The serotonin1A receptor partial agonist S15535 [4-(benzodioxan-5-yl) 1-(indan-2-yl) piperazine] enhances cholinergic transmission and cognitive function in rodents: a combined neurochemical and behavioral analysis. *J. Pharmacol. Exp. Ther.* 311, 190–203.
- Mohil, R., Kumar, D., Mor, S., 2014. Synthesis and Antimicrobial Activity of Some 1, 3-Disubstituted Indeno [1, 2-c] pyrazoles. *J. Heterocycl. Chem.* 51, 203–211.
- Moustafa, S.M.N., Elkanzi, N.A.A., 2021. Effect of the Newly Synthesized pyrazole, and pyrazolo pyrimidine derivatives on *Pythium aphanidermatum* (Edson) Fitzp. *Egypt. J. Chem.* 64, 8–9.
- Mukhtar, A., Shah, S., Hameed, S., Khan, K.M., Khan, S.U., Zaib, S., Iqbal, J., Perveen, S., 2021. Indane-1, 3-diones: As Potential and Selective α -glucosidase Inhibitors, their Synthesis, in vitro and in silico Studies. *Med. Chem.* 17, 887–902.
- Oliveira, A.F.C.d.S., de Souza, A.P.M., de Oliveira, A.S., da Silva, M. L., de Oliveira, F.M., Santos, E.G., da Silva, Í.E.P., Ferreira, R.S., Villela, F.S., Martins, F.T., 2018. Zirconium catalyzed synthesis of 2-arylidene Indan-1, 3-diones and evaluation of their inhibitory activity against NS2B-NS3 WNV protease. *Eur. J. Med. Chem.*, 149, 98–109.
- Ons, L., Bylemans, D., Thevissen, K., Cammue, B., 2020. Combining biocontrol agents with chemical fungicides for integrated plant fungal disease control. *Microorganisms* 8, 1930.
- J. I. Ofunne, "Bacteriological examination of clinical specimens", *Achugo Publ. Ama JK Recreat. Park. Owerri, Niger.*, 1999.
- Panahi, F., Yousefi, R., Mehraban, M.H., Khalafi-Nezhad, A., 2013. Synthesis of new pyrimidine-fused derivatives as potent and selective antidiabetic α -glucosidase inhibitors. *Carbohydr. Res.* 380, 81–91.

- Patel, A., Giles, D., Basavarajaswamy, G., Sreedhar, C., Patel, A., 2012. Synthesis, pharmacological evaluation and molecular docking studies of indanone derivatives. *Med. Chem. Res.* 21, 4403–4411.
- Pollard, P., Wortham, N., Tomlinson, I., 2003. The TCA cycle and tumorigenesis: the examples of fumarate hydratase and succinate dehydrogenase. *Ann. Med.* 35, 634–635.
- Protti, S., Dondi, D., Fagnoni, M., Albini, A., 2007. Photochemistry in synthesis: Where, when, and why. *Pure Appl. Chem.* 79, 1929–1938.
- Radwan, M.A., Alshubramy, M.A., Abdel-Motaal, M., Hemdan, B. A., El-Kady, D.S., 2020. Synthesis, molecular docking and antimicrobial activity of new fused pyrimidine and pyridine derivatives. *Bioorg. Chem.* 96, 103516.
- Rahjoo, V., Zad, J., Javan-Nikkhah, M., Gohari, A.M., Okhovat, S., Bihanta, M., Razzaghian, J., Klemsdal, S., 2008. Morphological and molecular identification of *Fusarium* isolated from maize ears in Iran. *J. Plant Pathol.*, 463–468.
- Reddy, K.H., Reddy, K.G., Reddy, D.V., 1985. Sensitive and selective spectrophotometric method for the determination of trace amounts of osmium with 1, 2, 3-indanetrione monothiosemicarbazone. *Microchim. Acta* 86, 319–330.
- Sarvesh, P.K., Nizamuddin, K., 2008. Synthesis and Antimicrobial Study of Novel 1-Aryl-2-oxo-indano [3, 2-d] pyrido/pyrimido [1, 2-b] pyrimidines. *Archiv der Pharmazie: Int. J. Pharmaceut. Med. Chem.* 341, 418–423.
- Shang, Y., Hasan, M., Ahammed, G.J., Li, M., Yin, H., Zhou, J., 2019. Applications of nanotechnology in plant growth and crop protection: a review. *Molecules* 24, 2558.
- Sharshira, E.M., Hamada, N.M.M., 2012. Synthesis, antibacterial and antifungal activities of some pyrazole-1-carbothioamides and pyrimidine-2 (1H)-thiones. *Am. J. Org. Chem.* 2, 26–31.
- Sheikhi-Mohammareh, S., Shiri, A., Maleki, E.H., Matin, M.M., Beyzaei, H., Baranipour, P., Oroojalian, F., Memariani, T., 2020. Synthesis of Various Derivatives of [1, 3] Selenazolo [4, 5-d] pyrimidine and Exploitation of These Heterocyclic Systems as Antibacterial, Antifungal, and Anticancer Agents. *ChemistrySelect* 5, 10060–10066.
- Sheldon, R.A., Arends, I., Hanefeld, U., 2007. Green chemistry and catalysis. John Wiley & Sons.
- Smilanick, J., Mansour, M., Margosan, D., Gabler, F.M., Goodwine, W., 2005. Influence of pH and NaHCO₃ on effectiveness of imazalil to inhibit germination of *Penicillium digitatum* and to control postharvest green mold on citrus fruit. *Plant Dis.* 89, 640–648.
- Srivastava, R., Khalid, A., Singh, U., Sharma, A., 2010. Evaluation of arbuscular mycorrhizal fungus, fluorescent *Pseudomonas* and *Trichoderma harzianum* formulation against *Fusarium oxysporum* f. sp. *lycopersici* for the management of tomato wilt. *Biol. Control* 53, 24–31.
- Tobiszewski, M., Marć, M., Gałuszka, A., Namieśnik, J., 2015. Green chemistry metrics with special reference to green analytical chemistry. *Molecules* 20, 10928–10946.
- Wu, W., Chen, M., Wang, R., Tu, H., Yang, M., Ouyang, G., 2019. Novel pyrimidine derivatives containing an amide moiety: design, synthesis, and antifungal activity. *Chem. Pap.* 73, 719–729.
- Xu, L.-L., Han, T., Wu, J.-Z., Zhang, Q.-Y., Zhang, H., Huang, B.-K., Rahman, K., Qin, L.-P., 2009. Comparative research of chemical constituents, antifungal and antitumor properties of ether extracts of *Panax ginseng* and its endophytic fungus. *Phytomedicine* 16, 609–616.
- Yu, B., Zhou, S., Cao, L., Hao, Z., Yang, D., Guo, X., Zhang, N., Bakulev, V.A., Fan, Z., 2020. Design, Synthesis, and Evaluation of the Antifungal Activity of Novel Pyrazole-Thiazole Carboxamides as Succinate Dehydrogenase Inhibitors. *J. Agric. Food. Chem.* 68, 7093–7102.
- Zhuang, J., Ma, S., 2020. Recent Development of Pyrimidine-Containing Antimicrobial Agents. *ChemMedChem* 15, 1875–1886.